THIRD ANNUAL CONFERENCE
AMERICAN SOCIETY OF BIOMECHANICS

THE PENNSYLVANIA STATE UNIVERSITY
UNIVERSITY PARK, PENNSYLVANIA

OCTOBER 21-23, 1979

TABLE OF CONTENTS

THE RECRUITMENT OF SKELETAL MUSCLE FIBERS DURING LOCOMOTION. Robert B. Armstrong, Oral Roberts University, Tulsa, OK 74171.

The purpose of this presentation will be to describe: 1) general relationships in the distribution of fiber types within and among mammalian locomotory muscles; and 2) how the fibers are recruited during locomotion as a function of speed and gait. Slow-twitch-oxidative (SO) fibers are generally concentrated in the deepest muscles within extensor groups, as well as in the deepest portions within individual muscles. Fast-twitch-oxidative-glycolytic (FOG) fibers have similar patterns of distribution. Conversely, fast-twitch-glycolytic (FG) fibers are most concentrated in the peripheral muscles within groups, as well as the peripheral portions within individual muscles. Several general conclusions may be drawn from experiments we have completed using glycogen loss in muscle fibers to estimate their utilization during locomotion: 1) deep muscles (primarily composed of SO fibers) within groups and the deepest portions within muscles (SO and FOG fibers), representing $<20\%$ of the total muscle group cross-sectional area, are active during slow running; 2) with increasing speed, a peripheral recruitment occurs within muscle groups and within muscles so that motor units with faster contractile properties and lower oxidative capacities are progressively activated; 3) at maximal running speeds nearly all fibers within extensor muscles, representing $>90\%$ of the total muscle group cross-sectional area, may be recruited; 4) discontinuities in the recruitment of the fiber types occur within some muscles when animals change gait (trot to gallop); 5) as FOG and FG motor units are recruited at higher running speeds, SO fibers continue to be activated; and 6) active total cross-sectional areas of extensor muscle groups are proportional to the forces the muscle group must produce, although this proportionality is not observed for individual muscles within the groups. I will attempt to integrate these and other observations into a unified concept of fiber type recruitment order in terrestrial locomotion, and discuss some of the remaining problems in our understanding of these mechanisms.

COMPARATIVE BIOMECHANICAL ANALYSIS OF THE SUBTROCHANTERIC AND INTERTROCHANTERIC OSTEOTOMIES

Alan L. Breed and Rajesh G. Narechania
Division of Orthopedic Surgery, University of Wisconsin Hospitals
Madison, Wisconsin 53792

The two most described rotational osteotomies for correcting the congenital hip dysplasia are the subtrochanteric and intertrochanteric. The literature abounds with the outlines of their operative techniques and the results. However, no work shows how the muscular relationships of the proximal femur, which undergoes rotation, changes after the surgical procedure. In the present paper we analyze the proximal femur for the muscular relationships after the surgical rotation.

The hypothesis is made that there is an abnormal rotational relationship of insertions of the muscles on the proximal femur with femoral anteversion. This hypothesis is made because the derotational osteotomy of the femur to correct anteversion has been performed at three different levels, supracondylar, subtrochanteric and intertrochanteric. The supracondylar level does not change rotational relationships of the gluteus maximus, iliopsoas, gluteus medius and gluteus minimus, the proximal femoral muscles. The subtrochanteric level changes the relationship of the gluteus maximus and the iliopsoas, but the relationship of gluteus medius and minimus to iliopsoas is not changed. Whereas the intertrochanteric osteotomy changes the rotational relationship of the gluteus medius and minimus with the iliopsoas, but not the relationship of the gluteus maximus with the iliopsoas.

An analytical model was developed to determine the functions of the iliopsoas and the gluteus muscles before and after the osteotomies. A normal femur was used to develop the model of an abnormal femur. The origins and insertions points of the iliopsoas, gluteus maximus, gluteus medius and gluteus minimus were identified on a cartesian coordinate system with the symphysis pubis as the origin.

Due to the internal rotation of the proximal end of the femur after the osteotomy, the resting lengths of these muscles are effected. For internal rotation of 30^{o}, the iliopsoas tightens by 6%; gluteus minimus by 7%; the gluteus medius decreases in length by 5%, and gluteus maximus by 10%. The muscles functions also change in flexion.

Our analytical results show that the subtrochanteric osteotomy can never release the iliopsoas and on the contrary it tightens the muscle which would therefore have increased tendency to re-dislocate the femur after the surgery. The effects of the gluteus minimus and medius are small compared to that of the iliopsoas. In the intertrochanteric osteotomy, the muscles involved are the gluteus medius and gluteus minimus. In this procedure the iliopsoas and gluteus maximus remain on the fixed distal fragment and thus the external rotatory components due to these muscles do not change. However it may still be tight in the patient with severe anteversion or CDH. As the proximal end of the femur is internally rotated, the gluteus medius is released. This decreases the external rotatory component and lowers the abduction component. The action of the gluteus minimus is similar to that of the gluteus medius. When the varus-osteotomy is performed the coxa femoral or the neck-shaft relationship changes. The lesser trochanter is advanced proximally and therefore the iliopsoas is released. Also the gluteus medius minimus decreasein length which given rise to increase in abduction torque. This helps in stabilizing the hip after the rotational osteotomy is performed.

A BIOMECHANICAL ANALYSIS OF LOAD LIFTING MOTIONS

Don B. Chaffin, Ph.D.
Arun Garg, Ph.D.

Ergonomics Laboratory
2254 G. G. Brown Laboratory
The University of Michigan
Ann Arbor, Michigan 48109

This paper presents a study of the motion dynamics involved in lifting maximum loads from floor to table height. Subjects selected their maximum loads psychophysically, i.e., by adding or subtracting lead shot from four different size containers which have an unknown weight added before each session. During both the initial and final trials in each session, stroboscopic photographs and force platform data were obtained.

These data are used in a seven link biomechanical model to determine how the articulation load moments vary with (1) load lifted, (2) size of contained, (3) practice, and (4) muscle strengths as determined by isometric tests. It is proposed that such information is important in determining lifting postures and load characteristics which produce strain/sprain injuries in industry.

"Kinematics Theory of Skeletal Joint Motion"

E. Y. Chao, Ph.D.
Orthopedic Biomechanics Laboratory
Mayo Clinic/Mayo Foundation

Abstract

Since the first systematic observation of human limb movements by Leonardo da Vinci, many experimental techniques and theories have been developed to analyze sophisticated human joint motion. In the wake of the present demand to apply motion measurement as a basic criteria to evaluate the functional performance of normal and diseased joints and the prognosis of various orthopedic reconstructive modalities, a comprehensive review and objective assessment of the major techniques currently being used to generate joint kinematic data are warranted.

The measurement of human joint motion can be divided into two main scopes: 1) the analysis of the joint articulating surface motion, and 2) the study of gross motion patterns. Either of these two types of motion requires a complete three-dimensional analysis since few joints in the human body possess true planar motion. If only joint rotation is of primary concern, the classic Eulerian angle concept is required to define the spatial orientation of human joints. The angular motion definition follows the gyroscopic mechanism and the advantage of such definition is that the final joint orientation is independent of the sequence of angular rotation. This new definition is very useful since it matches precisely the clinical definitions of joint motion. The general three-dimensional rigid body displacement can be defined by the Rodrigues vector (or screw axis) and the translation along the helical axis. Relative motion between two connecting rigid bodies can be deduced based on the same concept following the anatomical joint motion definition defined. The instantaneous spatial center of rotation can then be studied based on the theory of the Rodrigues vector. The articulating surface geometry can be mapped by a polynomial in two variables or by the technique of parametric surface patches. The joint contact surface area is determined based on a minimization process and articulating surface motion will be dependent on the general rigid body motion data of the joint segments.

Different methods of kinematic measurement of human joint motion will be presented. The basic theory, instrumentation, and data reduction techniques associated with each method are compared. The advantages and limitations in regard to these methods are discussed based on established results. Finally, potential clinical applications of joint motion data are outlined to stimulate further research in refining the experimental and analytical techniques so that reliable data based on the motion pattern of all human articulating joints can be established.

GAIT ANALYSIS IN THE STUDY OF HABITUATION TO TREADMILL WALKING

J. Charteris and J. C. Wall
Department of Human Kinetics
University of Guelph
Guelph, Ontario N1G 2W1
Canada

The purpose of this paper is to study the first ten minutes of exposure to treadmill walking by naive subjects. The angular kinematics and the temporal aspects of gait were analyzed to enhance the understanding of the habituation process. Towards this end habituation through a wide range of walking speeds was investigated.

METHOD

Thirty young adult male subjects, who were naive to treadmill walking, were each walked for ten minutes on a motorized treadmill. The subjects were split into five groups with the six subjects in each group walking at a given speed. The five relative speeds of walking selected were 0.55, 0.7, 0.86, 1.0 and 1.2, these figures being equivalent to the fraction of the subjects stature covered overground in one second. Using specially constructed footswitches and an electrically conducting coating on the treadmill belt, the patterns of foot contact were measured. Subjects were also filmed at 48 frames per second for the first 10 seconds of walking, from a standing start astride the moving belt and then for four strides at 30 secs, 1 minute, 2.5 minutes, 5 minutes and 10 minutes. Using a digitizer plate and minicomputer the films were analyzed to obtain the angular kinematic data.

RESULTS

The angular results from this study of 30 normal adult males accord with the findings of Charteris and Taves (1978) in their investigation of treadmill habituation of normal young adult females. Our addition of temporal measurements adds further confirmation to the implications of the prior study, namely that the initial accommodation to the exigencies of treadmill walking is swift and that a normalization of the gait pattern, after the initial bizarre steps are taken, essentially involves a "hunting" for greater stability of pattern. This is demonstrated in a decreasing stride to stride variability and a progressive tendency to replace the mincing step by a more relaxed, less energy expensive striding out.

Using constancy of gait as the measure of habituation it was found that at the slower speeds habituation is not complete after 10 minutes of treadmill walking. However at the faster speeds variation is less marked. The importance of these findings for rehabilitation is underscored by the fact that the gait of patients is typically slow. This means that habituation to treadmill walking should receive more than cursory attention where motorized treadmills are in operation in hospital settings and where measurements are being taken during the treadmill walk. Sufficient time must be allocated to habituation before these measurements are taken if the results are to be considered meaningful.

REFERENCE

CHARTERIS, J. and TAVES, C. The Process of Habituation to Treadmill Walking: A Kinematic Analysis. Perceptual and Motor Skills 47: 659-666, 1978

HUMAN GAIT ANALYSIS WITH A MINIATURE TRIAXIAL SHOE-BORNE LOAD CELL

by

R. Cheng, H. S. Ranu and A. I. King
Wayne State University, Bioengineering Center

For a number of years extensive studies have been carried out to evaluate the gait. In these studies all sorts of techniques have been used (e.g. force plates, shoe load cells etc.). But for the first time a miniature load cell has been developed which is so small that quite a number of these can be placed into different parts of the shoe without interferring with the normal gait. Thus making it possible to study not only the gait but also the force distribution under different parts of the foot. In this communication the use of such a load cell is described and data from the instrumented shoe is further correlated with the force plate.

A miniature triaxial load cell (7.9 x 19 x 19 mm approx.) which is capable of withstanding an axial load of 1300 N has been developed. It was strain gauged with EA-015EH-120Ω gauges for the vertical axis and WA-06-120Ω (Micro-Measurements, Romulus, Michigan) gauges for fore-aft and mediolateral axes. It was calibrated with a specially designed fixture which was capable of applying a minimum cross talk.

In order to correlate the data with the force plate, a lady's shoe was instrumented with such a load cell. Markers were placed on different parts of the shoe. The subject was made to walk on the force plate walkway and at the same time a high speed movie camera recorded the side view of the foot. Using a Vanguard motion analyzer the angle of shoe was measured at the instant of heel strike. Since it was necessary to take this angle into consideration in order to correlate the data with the force plate. The results show that the data from the shoe load cell is only off by less than 10% of the data from the force plate.

In order to study its clinical applicability, further evaluation was made with normal and abnormal subjects. This method of analyzing gait has been found to be simple, accurate and non-invasive.

BIOMECHANICS OF IMMUNE RESPONSES OF HUMAN POLYMORPHONUCLEAR LEUKOCYTES (PMNs), by Anthony T.W. Cheung *+ and Michael E. Miller *.

* Department of Pediatrics (E-6), UCLA School of Medicine, Harbor General - UCLA Medical Center, Torrance, California 90509.

\+ Department of Biology, Loyola Marymount University, Los Angeles, California 90045.

Increased appreciation of the importance of human immune responses against bacterial infections has led to increased understanding of mechanics in phagocytic functions and leukocytic locomotory characteristics. A major area of development is centered on the behavioral (locomotory) responses of normal and abnormal PMNs to known chemotactic gradients set up to duplicate disease conditions.

Preliminary investigations with visual assays in the study of movements of human PMNs have been explored. We are in the process of perfecting a visual assay, utilizing micro-videotaping techniques in the investigation of the locomotory responses and functional characteristics of human PMNs (normal as well as abnormal) to known chemotactic gradients.

Correlation of such quantitative information with existing information from membrane deformability (elastimetry) and modified Boyden chamber studies will give a more complete characterization of the chemotactic response phenomenon.

Normal PMNs, PMNs with locomotory defects induced by pharmacological agents and PMNs from patients with known deficiencies are used. A chamber (plexiglas) which can establish a chemotactic gradient for PMNs to respond to, has been developed. Such a slide-chamber serves to provide a means for microscopic visualization and documentation of cellular responses to the gradients. The chamber has been successfully tested for effectiveness and consistency and definite positive and negative chemotactic responses have been recorded. Available data have been analyzed and interpreted.

Instrumentation development plays an important role in this investigation. Quantitative documentation is a necessity and is the only means to account for all the locomotory responses and the behavioral characteristics to chemotactic gradients. Such a development is still in progress. We have incorporated into our micro-video system specialized optics, high-speed movie and time-lapse movie capacity. Such a set-up can provide, on a time-dependent basis, quantitative documentations at magnifications and resolutions sufficient to reveal structural and behavioral (microscopical) characteristics of human PMNs, as a response to known chemotactic agents.

The research is funded by NIH Grant 5-R01-HL-20002 - 03 and NIH (MBS) Grant 5-S06-RR-08140.

Relationships between tethered and free swimming the front crawl stroke.
Albert B. Craig, Jr. and William F. Boomer. Dept. of Physiology, School of Medicine and Dentistry, and Division of Sports and Recreation, Univ. of Rochester, Rochester, New York 14642.

Swimming against different retarding forces (partially tethered swimming) or an infinite force (completely tethered) has been a useful tool with which to study the biomechanics and physiology of swimming. However, the results of such experiments are difficult to relate to free swimming. The current studies of tethered swimming yield data which correlate well with the subjects' maximal free swimming velocities (v max.). Nine male and nine female swimmers who had just finished their competitive season participated. The best time for swimming 100 yards was known for each. The v max. was determined by having the subject swim as fast as possible for 10 m for the males or 8 m for the females. The times for such swimmers varied between 5 and 6 seconds. In the partially tethered swimming experiments the subjects made repeated swims pulling against 8 different retarding forces (D_A) (range 1.8 to 10 kg for females and 3.3 to 13 kg for males). The constant velocity at which the weight was lifted (v wt.) was measured for 5-6 seconds. In other experiments the mean force which would be developed when the subject was completely tethered (F_t) was measured by integrating the output of a force transducer for five complete strokes and dividing the integrated signal by time. The times for these swims were also 5-6 seconds.

The average v max. for the males was 1.78 and for the females was 1.47 m/sec. In both groups there was a direct relationship between the subject's best time for a 100 yard race and the v max. (r=.81). As the D_A was increased, the v wt. decreased, and the relationship could be described by v wt. = $A(D_A) + B$. The average A was -.112 for the males and -.144 m/sec/kg for the females. The calculated forces at v wt. = 0 (D_A max.) were 12.0 and 7.6 kg for each group respectively. Although the F_t was somewhat greater than this calculated value, they were directly related. As both v wt. and D_A were known, the maximal power output ($\dot{W}$) could also be calculated. This value was 4.1 for the males and 2.1 kpm/sec for the females or 12.6 and 6.3 watts.

There was a direct positive correlation between v max. and D_A max., $\dot{W}$, or F_t (r for males, .70, .86, and .81; for females, .79, .73, and .82). The correlations were somewhat better when the values were normalized for surface area. There was no relationship between the constant A which reflects D_A/V and the v max.

It was apparent that measurements of F_t and calculations of D_A max, and $\dot{W}$ during partially tethered swimming indicate major attributes of the swimmer. Although these factors were 50-60% less for the female than the male, the v max. of the females was 83% of the male value. The slope of the line relating v and D_A was greater for the females. This slope probably reflects the lesser energy costs of swimming for the females. This latter observation suggests that both maximal power output and proficiency of swimming are important in determining v max.

Design and Materials of Feather Shafts: Very Light, Rigid Structures.

Donald G. Crenshaw
Department of Zoology
Duke University
Durham, North Carolina 27706

The shafts of flight feathers resist aerodynamic loads imposed by flight. The broad design criteria are straightforward: 1) resist breaking, 2) resist excessive bending, 3) be as light as possible. Feathers meet these criteria by means of "sandwich" construction. A rectangular tube of compact keratin surrounds a pith of spongy keratin.

Intact shafts and shafts with the pith removed were tested by three-point bending with the dorsal surface in compression, thus partially simulating the direction of in-flight bending loads. Feathers were tested to failure. Failure was always by buckling of the compression surface, often accompanied by splitting of the tension surface. The intact shafts failed under a bending moment of $1.5 \times 10^{-1} N \cdot m$. The altered shafts failed at $5.0 \times 10^{-2} N \cdot m$. The reduced strength of the altered shafts is accounted for by several factors. Removing the pith lowers the second moment of area from $5 \times 10^{-13} m^4$ to $2 \times 10^{-13} m^4$. Maximum stress at failure was $2.3 \times 10^{8} N \cdot m^{-2}$ in tension and compression for both whole and reamed shafts. Tensile tests of compact keratin show the ultimate tensile stress to be $2 \times 10^{8} N \cdot m^{-2}$. Tensile tests of whole shafts indicate that spongy keratin contributes very little to tensile strength. Because buckling and tensile failure occur at the same stress, no part of the feather is "overbuilt". The spongy keratin resists the low tensile and compressive stresses which occur in the center of a bent shaft. The spongy keratin provides a considerable increase in strength for a slight increase in weight. The density of compact keratin is $6 \times 10^{2} kg \cdot m^{-3}$ yet the density of intact shafts is $5 \times 10^{2} kg \cdot m^{-3}$.

The material properties of feather keratin show it to be a strong, light substance. The arrangement of compact and spongy keratin in the shaft shows that the materials are well placed in the structure to fulfill the criteria mentioned above. Detailed study of the aerodynamics of bird wings will allow better estimates of the forces acting on the feathers and hence sharpening of the criteria for how feathers resist the forces.

Whole Body and Segment Center of Mass Determination from Kinematic Data

A. Dainis

Biomechanics Laboratory, Dept. of Physical Education
University of Maryland, College Park, Md. 20742

ABSTRACT

A technique is described for determining the location and motion of the center of mass of a rotating multiple link system from displacement data provided that the motion of the center of mass can be expressed as a polynomial function of time. It is also demonstrated that for a link system the center of mass location determines a configuration-independent relationship between the segmental masses and the locations of the segment centers of mass. This provides a method of measuring, from kinematic data, the segmental parameters of mass if their locations of center of mass are specified, or conversely, locations of center of mass if their masses are specified.

A computer program has been written to utilize coordinates digitized from any number of frames of cinematographic film for the case of link systems moving in two dimensions under the influence of gravity. Application is made to the motion of mechanical link systems and the human body. The results show good agreement with those obtained by independent methods, and indicate the particular usefulness of the technique in situations of free fall and weightlessness.

SIMULATION OF MODIFIED HUMAN AIRBORNE MOTION

Jesús Dapena. Biomechanics Laboratory, Department of Exercise Science, University of Massachusetts, Amherst, MA., 01003.

Many sports activities involve relatively prolonged periods of time during which the body is airborne. The outcome and/or the mode of execution of the airborne phase may have a bearing on the value of the performance. There is a need for a more thorough understanding of the mechanics of the airborne phases of sports activities.

Airborne motion is characterized by certain mechanical properties which make it unique. Ignoring air resistance, the parabolic path of the center of mass (c.m.) is completely determined from the instant when the body is free in the air, and the angular momentum of the body about its c.m. is fixed. However, the rotational behavior is not completely determined if the distances between different parts of the body (and therefore the inertial properties of the body) can change. The rotational behavior of an airborne athlete can be modified by changing the orientations of body segments relative to each other.

The purpose of this study was to link a 3-D analysis of actual human body motions under free-fall conditions, with the prediction of the modified motions produced by diverse prescribed alterations. The prescribed alterations consisted of selected modifications of the configuration history of body segments relative to the upper trunk during the airborne phase.

The method was divided into two stages: (1) analysis of the actual motion, and (2) generation of the simulated motion. The output from Stage 1 was used as input for Stage 2 after introducing prescribed alterations in it.

Error in the method was reflected in two ways: (1) translation error, i.e., error in the location of the c.m. of the whole body; and (2) rotation error, i.e., error in the rotation of the upper trunk. Overall, the period of validity of the method was estimated, on the basis of error measurements, at approximately .6 to .8 sec. of airborne motion, although this figure could vary for different activities or subjects.

Other researchers have previously developed methods of simulation of 2-D and 3-D human airborne motions, using body models of diverse complexity. In some cases the simulations represented modifications of actual body motions. The present method is the first one to combine the analysis of 3-D airborne motions of a multisegmental human body with the prediction of modified body motions. The method permits the modification of initial conditions and/or segmental orientation patterns of the diverse segments relative to the upper trunk. The method is designed to be used as a tool to provide a better understanding of human airborne motion.

THE COST OF LOCOMOTION - GASTROPOD CRAWLING

Mark Denny
Department of Zoology
University of British Columbia
Vancouver, B.C.

The cost of locomotion of vertebrates has been extensively studied, and general trends have been described[1]. Invertebrate locomotion, however, has received far less attention. This study reports on the cost of one form of invertebrate locomotion; the adhesive crawling of gastropods.

Gastropods crawl using a single appendage - the foot. The power for locomotion is provided by a series of muscular waves present on the foot's ventral surface. The movements are coupled to the substratum by a thin (10-20μm) layer of mucus. This mucus acts as a glue which allows the animal the advantage of adhering to the substratum. However, the adhesiveness of the mucus must be overcome for the animal to move. The detailed mechanism and cost of this form of locomotion was studied in the terrestrial slug, Ariolimax columbianus.

The external power of locomotion, P_e, was measured by inducing slugs to crawl across a small force transducer incorporated into a horizontal surface. This measured power can be accurately explained by a theoretical model which relates the movements of the foot (measured with a video tape recorder) and the unusual physical properties of the pedal mucus[2]. At a typical crawling velocity, V, of 2×10^{-4}m/sec, $P_e = 3.2 \times 10^{-3}$ W/kg. The slope of the P_e/V curve rises with increasing velocity. The net oxygen consumption due to locomotion was measured simultaneously with crawling velocity in a differential respirometer. From these data the internal power of locomotion, P_i, and overall cost of transport were calculated. P_i rises linearly with V, with a value of 0.19 W/kg at 2×10^{-4}m/sec. The slope of the P_i/V curve gives the cost of transport, which here is 952 J/kg/m. This cost is over ten times higher than that measured for any other form of locomotion (Figure). This high cost of locomotion is primarily attributable to the metabolic cost of producing pedal mucus which was estimated at 32.5% of the internal cost of locomotion, P_i. The high cost of movement is secondarily attributable to the direct muscular cost of moving over the mucus. This was estimated to range from 8.5% of P_i at a low V to 26.0% of P_i at the maximum observed crawling velocity. The efficiency of locomotion (P_e/P_i) is 0.017 at 2×10^{-4}m/sec, rising to 0.052 at the maximum velocity of 2×10^{-3}m/sec. These values are similar to those for a person running horizontally[3].

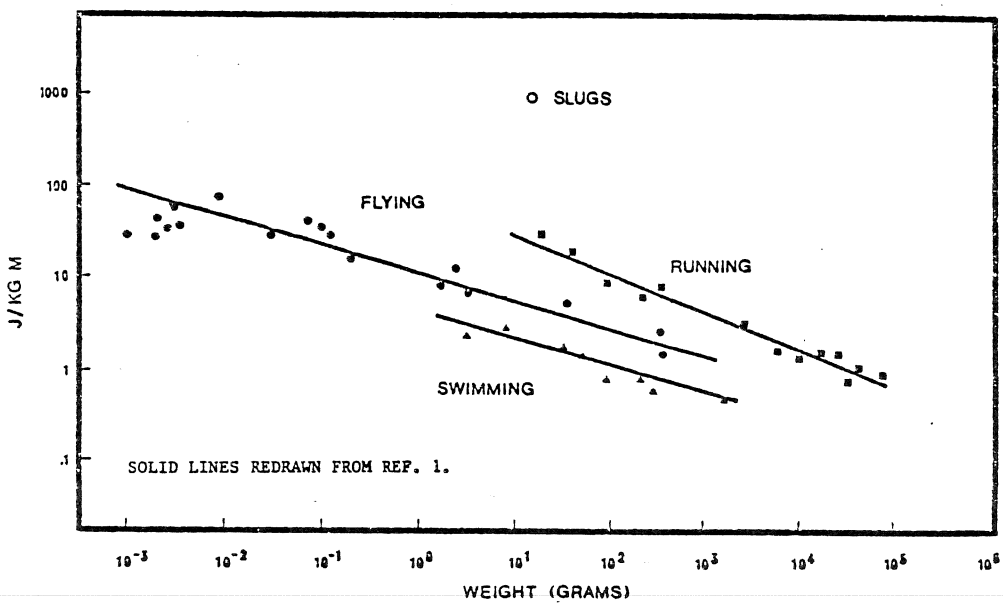

In summary, the necessity of producing and crawling over pedal mucus renders this form of locomotion costly. Presumably this adhesive crawling evolved so that the advantage of adhering to the substratum acts to offset this cost. While costly, the crawling of A. columbianus is not inordinately inefficient.

1. Schmidt-Nielsen, K. 1972. Science 177:222-228.
2. Denny, M.W. 1978. Biorheology 15:460.
3. Tucker, V.A. 1973. in Comparative Physiology. Bolis, L., Schmidt-Nielsen, K., and Maddrell, S.H.P. (eds.) North-Holland.

POWER OUTPUT AS A FUNCTION OF LOAD VARIATION IN OLYMPIC AND POWER LIFTING

John Garhammer, Biomechanics Laboratory, Department of Kinesiology, UCLA, Los Angeles, CA. 90024
Thomas McLaughlin, Biomechanics Laboratory, Auburn University, Auburn, AL. 36830

Strength and power are of major importance in competitive lifting while weight training is consistently used as a means to develop these qualities in other athletes. Squats, cleans, snatches, and deadlifts are generally accepted as being productive training lifts for athletic events which require a coordinated total body effort. No data has been found in the literature regarding power production during a squat or deadlift. Likewise, no data has been found regarding the variation in power output as a function of the weight lifted in any of the above four lifts. The purpose of this study was to collect information on power production during these lifts and to examine its variation with load changes in each of the movements. Data were obtained from 16mm films taken @ 50 fps at the 1974 and 78 U.S. National Powerlifting Championships, 1975 and 77 U.S. National Weightlifting Championships, 1977 and 78 Las Vegas International Meets, and the 1978 World Weightlifting Championships. Situations were picked for study where a given lifter made two successful lifts of one type. The highest weight lifted in a meet was considered a 100% effort for that occasion. The method used to calculate power production for snatches and cleans has been described previously and includes both vertical and horizontal work done in lifting the barbell along with work done in lifting the body's center of mass.* This method was also used to obtain power output for squats and deadlifts with lift completion taken at the instant the barbell reaches maximum vertical elevation. A total of 41 pairs of lifts were available for analysis, many of which included a world or national record. Results showed that power outputs for athletes of similar bodyweights were two to three times higher in snatches and cleans than in squats and deadlifts. The primary reason being the longer duration of lifting effort in the latter two movements. In the squat and deadlift analyses the power output was found to be considerably lower for the 100% effort, and in some cases more than 50% lower than for a 90% effort. Typical squat values for a superheavyweight lifter were 900 watts at maximum effort (4112 N/ 923 pounds) vs. 1259 watts for a 93% effort. Differences in power output for snatches and cleans were not as great, primarily due to smaller load variations and the necessity of fast movement for success. However, power production was again consistently lower for the maximal efforts. A lightheavyweight lifter produced 2173 watts with a 100% snatch (1396 N/ 314 pounds) and 2298 watts at 98%. Information of this type should be very important to both competitive lifters and athletes choosing training lifts and weights to be used for the development of strength and/or power. In squats and deadlifts strength appears to be the key factor due to the heavier weights typically handled, since power output was consistently lower in these lifts than in cleans and snatches. Power generation was greater in all of the above lifts at submaximal loads. Strength vs. power requirements of the athletic event being trained for must be considered in light of the above information in order to properly balance these components in a weight training program if optimal benefits are desired.

*Garhammer, J. Power Production by Olympic Weightlifters. (Accepted for publication in Med. Sci. Sports, 1979.)

PRIMARY RESTRAINT IN THE ISOLATED KNEE JOINT DURING TRAUMATIC POSTERIOR DRAWER

Roger C. Haut, Biomedical Science Department
GM Research Laboratories, Warren, Michigan 48090

Frontal impact on the lower leg with the knee flexed at 90° results in posterior tibial displacement. When the motion is excessive, injuries to the knee can occur by avulsion fracture or central tearing of the posterior cruciate ligament (PCL) [1]. Butler [2] has shown that at physiological levels of deformation (< 0.5 cm of drawer) the PCL provides 89% of the total force and 87% of the dynamic stiffness, but in tests to trauma, the force-displacement response of the isolated knee is smooth and linear only to approximately 1.4 cm of drawer. At larger deformations the response is complicated by plateaus or slight unloadings indicative of either partial or complete rupture of the PCL with subsequent loading of secondary supporting structures up to total joint collapse at 2.3 cm.

The objective of this study was to determine the behavior of the PCL and secondary supporting structures of the knee (i.e., anterior cruciate ligament, collateral ligaments, and posterior capsule) at traumatic levels of posterior drawer with the joint flexed at 90°. Dynamic tests were conducted on 6 isolated cadaver knees obtained through the gross anatomy program at the University of Michigan School of Medicine. In the preparation all superficial tissue was removed leaving the intra-articular and collateral ligaments, the meniscus, and the posterior capsule. A 5 cm posterior drawer was induced at a rate of 180 cm/s. Responses of contralateral knees were compared with only the PCL in one joint and the standard preparation in the other.

The results of these experiments indicate that the ultimate mechanical properties of the isolated knee subjected to posterior drawer (i.e., 2.76 ± 0.75 kPa at 2.31 ± 0.68 cm) were not influenced by removal of secondary supporting structures (2.91 ± 1.42 kN at 2.19 ± 0.78 cm). The structural stiffness of the joint (1.65 ± 0.24 kN/cm) actually increased after removal of the secondary restraints (1.79 ± 0.35 kN/cm). Although the average change in stiffness between the test groups was not statistically significant, comparative contralateral knee tests showed an average increase of 15% in 5 of 6 cadaver tests. In 2 cadaver specimens, a slight plateau or unloading of the force-displacement response was associated with bone fractures in tests on the contralateral knees.

These experiments indicate that the total ligamentous stability of the isolated flexed cadaver knee is provided by a single ligament, the PCL, even at traumatic posterior drawer. However, secondary restraints may slightly influence the orientation of the PCL and contribute to structural joint stiffness. A sign of premature unloading or a plateau in the force-displacement response may be associated with incipient bony microfracture rather than partial rupture of a ligamentous structure [3].

References:

1. Viano, D. C. et al (1978), "Bolster Impacts to the Knee and Tibia of Human Cadavers and a Part 572 Dummy," Proc. 22nd Stapp Car Crash Conf. Ann Arbor, MI.

2. Butler, D. L. et al (1977), "Ligamentous Contributions to AP Stability of the Knee," 1977 Biomechanics Symposium, A.S.M.E., AMD-Vol. 23:217-220.

3. Noyes, F. R., E. S. Grood (1976), "The Strength of the Anterior Cruciate Ligament in Humans and Rhesus Monkeys--Age Related and Species Related Changes: J. Bone Jt. Surg., 58-A:8, 1074-1082.

DEVELOPING A STRATEGY TO IDENTIFY THE TECHNICAL FACTORS LIMITING PERFORMANCE. James G. Hay, Biomechanics Laboratory, Department of Physical Education, University of Iowa, Iowa City, Iowa

Although improving the performance of motor skills is one of the ultimate aims of research in the biomechanics of sport, very few attempts have been made to develop a systematic approach for this purpose. The purpose of this paper is to review the attempts which have been made and to present a progress report on an alternative procedure.

The attempts which have been made to improve performance via biomechanical analysis fall into two broad categories. The first includes all those studies in which statistical procedures have been used to identify factors related to the quality of performance. The second includes those in which mathematical modelling has been used to study the effect that variation in selected factors has on the performance or to determine that technique which maximizes the performance. Those attempts involving statistical procedures -- by far, the larger number to the present time -- have usually been lacking in several respects. They have almost invariably lacked a theoretical basis for the selection of the independent variables to be studied; they have often involved the use of less subjects than is adequate for the statistical procedure used; and they have rarely made provision for determining an order of priority among the variables found to be important.

The alternative procedure presented consists of three steps: (1) the development of a deterministic model linking the performance to the underlying technical factors upon which it is based, (2) the gathering of data on a representative sample and (3) the analysis of that data to identify and order those technical factors which limit the quality of the performance.

The development of an appropriate deterministic model provides a rigorous basis for identifying the factors (or variables) which should be included in the analysis and those which, because they are either noncausal or redundant, should be excluded. A deterministic model which can be used in the analysis of a wide range of skills is proposed.

The number of subjects per independent variable is often a source of concern in studies in which a large number of variables is involved and/or in which the availability of subjects or the time to obtain the data on one subject is a problem. The effect of sample size on the validity of the proposed procedure has been studied by comparing the results obtained using samples of varying sizes ranging from 50 to 194 subjects.

The crucial data analysis step of the procedure has undergone many changes in the course of its development -- changes designed primarily to overcome the problems of suppression and multi-collinearity. The proposed compromise solution to these problems is based on both mechanical and statistical considerations.

The development of a rigorous procedure to identify and evaluate limiting factors is a vast, multi-faceted problem and, while some progress has been made towards its solution, there is much that remains to be done.

Kinetics of Postural Control in Man

Keith C. Hayes
Patrice L. Weiss
Warren Darling
Department of Kinesiology
University of Waterloo
Waterloo, Ontario, N2L 3G1

Maintenance of equilibrium in man is accomplished through the combined influences of centrally generated commands to postural musculature and sensory feedback from peripheral receptors. In the event of predictable perturbations to the musculo-skeletal kinematic linkage, as occurs when a voluntary arm movement is initiated, centrally generated stabilizing muscle torques serve to minimize the disturbance to the center of gravity. In the present study an attempt was made a) to identify the patterns of stabilizing postural torques in axial and lower limb musculature that precede bilaterally symmetrical arm movements, b) to predict these patterns of muscle activity on the basis of the dynamics of the forthcoming movements, and c) to determine the energetics of postural maintenance in the five-segment kinematic chain.

Cinematographic data (Bolex H16,50fps), force-platform, accelerometer (Endevco 20G piezoresistive), and telemetered EMG records (Biocom 270:20-150Hz) from seven muscle groups, were obtained from five healthy female subjects performing three different bilateral arm movements: i) flexion, ii) flexion with 2kg load, iii) extension. Force-platform, accelerometer and EMG data were stored on magnetic tape (HP. 3960 FM 0.2-625Hz) prior to A-D conversion and subsequent processing in a Nova 2/10 minicomputer. Dominant muscle torques were computed from the low-pass filtered (double pass of Butterworth second-order; 5Hz) kinematic data using Newtonian rigid-body mechanics and standard anthropometric data. The temporal relationships between the torque-time histories and the linear envelope EMG signals were established and finally the energetics were calculated. Instantaneous segmental energies were determined from the equation:

$$E_i = \tfrac{1}{2}m_i v_i^2 + \tfrac{1}{2}I_i\omega_i^2 + m_i g h_i$$

and the power flow, attributable to muscle torques ($M.\omega_i$) and joint reaction forces ($\vec{F}_i.\vec{v}_i$), was partitioned.

Consistent patterns of anticipatory postural activity occurred in all of the muscle groups prior to each of the different movements. The earliest activity preceded the onset of deltoid muscle activity and arm acceleration, by more than 50 msec. The pattern of onset of muscle activity and the time histories of muscle activity were found to be predictable from the dynamics of the forthcoming movement. Evidence was also found of functional synergies among certain muscle groups, notably erector spinae and hamstrings; quadriceps and rectus abdominus (cf. Nashner, 1978).

These results indicate that the preparatory stabilizing activity in trunk and lower limb muscle groups that constitute the centrally generated "postural motor program" is organized in simple, but strict, accordance with the dynamics of the forthcoming movement. Moreover, the activity is predictable if the movement dynamics are specified. This preprogrammed postural activity appears to increase the stiffness of the musculo-skeletal linkage, thereby minimizing the disturbance to the kinematic chain and the energy demands of maintaining equilibrium. The newly identified means of predicting "appropriate" patterns of postural muscle activity has important clinical ramifications in the assessment and treatment of patients with cerebellar or basal ganglia pathologies, in which balance problems are experienced, and for the improvement of therapeutic procedures which currently rely solely upon facilitation from the sensory consequences of passive movement.

The Mechanical Properties and Locomotory Functions of Eel Skin

Mary R. Hebrank
Department of Zoology
Duke University
Durham, NC 27706

The skin of the American eel Anguilla rostrata is composed largely of a crossed array of collagen fibers oriented at an angle of 45° with the long axis of the fish. The volume fraction of these fibers remains fairly constant (66%) in eels ranging from 20-64 cm. in length. Uniaxial and biaxial testing of eel skin have been used to assess the role of the collagen fibers in the locomotory functions of the skin.

Although the geometry of the fibrillar arrangement predicts that the skin should be isotropic in the circumferential and longitudinal directions of the fish, it is an order of magnitude stiffer in the circumferential direction. The mean terminal elastic modulus (the elastic modulus in the steep part of the stress-strain curve) in the circumferential direction is 14.6 MNm^{-2}, while that for skin stressed in the longitudinal direction is 3.5 MNm^{-2}. The elastic modulus for skin stressed uniaxially in the direction of the fibers is about 0.16 GNm^{-2}. Within the range of in vivo extensions skin stressed in the longitudinal direction behaves like a pure fiber system while skin stressed in the circumferential direction does not. Skin which is stiffer in the circumferential direction may be important in resisting transient pressurization during swimming.

The mechanical behavior of the skin indicates that the skin may act as an external tendon, transmitting forces arising in the axial musculature down the length of the fish to the tail. The collagen fibers within the skin may also play an important role in torsion resistance when the eel executes its peculiar "corkscrew" motion.

HUMAN SPINAL COLUMN MECHANICS AND INJURY MODES FOLLOWING INITIATION OF SEAT EJECTION

Leon E. Kazarian, Dr. Ing.
Aerospace Medical Research Laboratory
Aerospace Medical Division, Air Force Systems Command
Wright-Patterson Air Force Base, Ohio

ABSTRACT

High performance military aircraft are equipped with an ejection seat that allows an aircrewman to escape immediately following damage or command initiation. Whatever the reason, when a decision is made to abandon an aircraft, the ejection seat provides a reasonable chance of successful escape. With the increasing complexity of high performance tactical aircraft being introduced into the operational service, it has become progressively more difficult to insure non injurious emergency escape.

The ejection sequence may be divided into the following events: Preejection positioning, catapult intiation and stroke, main parachute snatch, and ground landing impact. During any of these events, aerodynamic and inertial forces result in orthopaedic disorder. Sustained injuries may involve the extremities or the spinal column. The problem of extremity injury during egress is recognized as a continuing one especially at airspeeds greater than 350 KIAS.

This paper deals with spinal column trauma. Spinal column trauma has been a problem since the early development of emergency escape devices and has increased in frequency at severity over the past ten years.

There exists a lack of knowledge concerning the subject of spinal injuries associated with ejection. Many spinal injuries are of a minor nature, where as others are immediately fatal. Between these two extremes exists a wide variety of spinal column lesions. Fractures of the spinal column may be classed by various methods both with respect to causation and to the anatomical character. The type of spinal fracture is determined primarly by the dynamic force sustained. Forces producing hyperextension, hyperflexion, compression, torsion about the longitudinal axis are the main causes of spinal fracture.

The purpose of this overview is to contribute further to our understanding of traumatic vertebral body and intervertebral disk lesions following initiation of the ejection sequence. The various frames of reference of the open ejection seat are identified at human body kinetics within that framework characterized. The frequency, type, and severity of spinal column injury are classified and the modes of injury delineated.

COMPARISON OF HUMAN SKULL AND SPHERICAL SHELL VIBRATIONS-- IMPLICATION TO HEAD INJURY MODELING

Tawfik B. Khalil, Ph.D. and David C. Viano, Ph.D.
Biomedical Science Department
General Motors Research Laboratories
Warren, Michigan 48090

Abstract

Spherical shell models have been formulated as geometric approximations of the human head. By insuring geometrical and material similarity between the shell model and human head, impact response and skull fracture studies were expected to yield results in close agreement with model predictions. This, however, was not the case. Model predictions of skull fracture loads were typically twice the observed level.

A comparison was made between the resonant frequencies of two dry human skulls and corresponding spherical shell models. Poor agreement was observed with the frequency of the shell resonances about twice those of the skulls. A vibrational analysis of the model revealed that the uniformity of the spherical shell approximately doubles the effective stiffness and resonant frequencies as compared to the dry human skull. The elastic modulus of the spherical shell model was subsequently adjusted so that the resonances of the model could be brought into closer agreement with those of the human skull. An "effective" modulus was synthesized which was 50% lower than the material property of human cranial bone. Interestingly, this adjustment also brought model predictions of skull fracture into closer agreement with available human cadaver data.

STRENGTH EVALUATION OF ANTERIOR AND POSTERIOR CRUCIATE LIGAMENT RECONSTRUCTION IN THE RHESUS MONKEYS

Narechania, R.G.; Clancy, W.G.; Rosenberg, T.; Gmeiner, J.G.
Division of Orthopedic Surgery, University of Wisconsin Hospitals
Madison, Wisconsin 53792

Introduction: Patellar tendon substitution for anterior cruciate ligament and posterior cruciate ligament instability has recently gained a great deal of attention. The object of our study was to document biomechanically the adequacy of our reconstruction technique in Rhesus monkeys.

Methods and Materials: Twenty Rhesus monkeys age range corresponding to young adult human, underwent a modified Eriksson procedure for the anterior cruciate reconstruction. Three were sacrificed at intervals of 8 weeks, 3, 6, 9 and 12 months postoperatively. At surgery the anterior drawer was measured prior to the sacrifice of the anterior cruciate ligament and again after the patellar tendon substitution. At the selected sacrifice time, the anterior drawer was remeasured by means of strain gage transducers on a knee stress apparatus. The knee joints were then completely dissected except for the reconstructed anterior cruciate ligament and the contralateral normal anterior cruciate ligament. The normal and the reconstructed ligament preparations were then tested on the material testing system, MTS-30MP. The rate of deformation was 1 cm per second.

The posterior cruciate ligament reconstruction was performed in 10 Rhesus monkeys utilizing the patella tendon free graft. This graft is comprised of the medial 1/3 of the patellar tendon, the patellar bone and the tibia bone. Two were sacrificed at intervals of 8 weeks, 3, 6, 9 and 12 months. One was utilized for microangiography and the other for MTS testing.

Results and Discussion: Our results showed that there was essentially no significant increase in laxity at surgery after cruciate ligament substitution. All monkeys were placed in a cylinder cast with 60^{0} of knee flexion for 6 weeks.

At appropriate sacrifice intervals, there was no significant increase in the anterior drawer as measured on a knee stress apparatus.

Measurement with MTS for the ultimate strength of the normal control ligament and the reconstructed ligament showed that the failure occurred within the substance of the ligament or tendon substitution. Our study has shown that the strength of reconstructed knees against the respective contralateral sides rises with time, but does not reach the strength of the normal ligament.

The tensile strength of the control anterior cruciate ligament averaged 650 newtons, the posterior cruciate 450 newtons, and the medial 1/3 of the patella tendon 300 newtons.

Tensile testing revealed that the patella tendon substitutes for both the anterior and the posterior cruciate ligaments retained approximately 80% of their inherent tensile strength at nine months and one year. The anterior cruciate-patella tendon substitute underwent significant hypertrophy in three of eight cases between 9 and 12 months. The posterior cruciate-patella tendon substitute underwent significant hypertrophy in one of two cases between 9 and 12 months.

Gait Efficiency and Exercise Intensity in Spastic Children*

Authors: David H. Nielsen, LPT, Ph.D.
David J. Smyntek, LPT, M.A.
Gary L. Smidt, LPT, Ph.D.
Physical Therapy Education (319-356-2968)
The University of Iowa
Iowa City, Iowa 52242

Abstract

There is a paucity of information concerning gait efficiency in cerebral palsied children. Presently it is unknown if the efficiency of gait changes with different walking velocities or if the cerebral palsied child naturally selects an efficient walking velocity. Because energy requirements can be a limiting factor in pathological gaits, the determination of the relative exercise intensity of gait is therefore an important consideration.

The purpose of this study was to determine the effect of walking velocity in milding involved spastic cerebral palsied children on three measures of gait efficiency: 1. gross efficiency (positive work/V_{O_2}), 2. distance efficiency ($\dot{V}_{O_2}$/velocity), 3. technique efficiency (harmonic ratios derived from acceleration data) and relative exercise intensity (% MHR).

Fifteen ambulatory spastic cerebral palsied children served as subjects. Self-selected velocity (S-SV) was measured during a standardized five minute walk. $\dot{V}_{O_2}$, HR, acceleration and vertical displacement of the body center of gravity were determined for three different velocities (15% < S-SV, S-SV, 15% > S-SV.

The results indicated that V_{O_2}/meter of the cerebral palsied children was approximately 200% of that of normal persons while walking at a 30% slower S-SV. Analysis of variance indicated significant increases in % MHR (59% 63%, 66%) with walking velocity. Although gait efficiency was impaired, the group differences in the three measures of gait efficiency were not statistically significant for the three walking velocities. V_{O_2}/meter and $\dot{V}_{O_2}$ appeared to be the best discriminators of gait performance.

*Supported by a grant from the National Easter Seal Research Foundation.

STARFISH DERMIS: AN ORTHOGONAL COLLAGEN ARRAY

Patricia L. O'Neill
Department of Zoology
Duke University
Durham, North Carolina 27706

Echinoderms of the class Asteroidea (starfish) have a thick collagenous dermis in which the skeletal ossicles of $CaCO_3$ are embedded. For many years, the collagen fibers were described as a random feltwork. This structural assumption seemed inadequate to account for properties of the body wall noted during behavioral observations of starfish, eg, rigidity during normal locomotion and extreme flexibility in bending and torsion. In this study, the dermis of the dorsal (aboral) body wall of the arm of the asteroid Echinaster spinulosus was examined.

Frozen sections of the dermis viewed in polarized light revealed that the collagen fibers form a highly organized fibrous gridwork with principle axes coincident with the longitudinal and transverse axes of the arm. The fibrous tracts average 0.30 to 0.05 mm in diameter. The skeletal ossicles are contained within the spaces of the orthogonal network. Some of the spaces, accounting for 10 to 12% of the total tissue volume, are left as open voids through which the papulae (dermal gills) exit. Fibers frequently deviate from the principal axes to make detours around ossicle and papular holes. The connections between ossicles and dermis are intimate; the collagen fibers invade the interstices of the calcareous meshwork of the ossicles. Crossovers between fiber tracts often form junctions which are tight and appear to be interwoven. Although the intact tissue cannot be teased into separate fibers, microscopic examination indicates that the fibers are probably continuous. Unlike vertebrate collagen, the fibers do not appear wavy when relaxed.

Uniaxial tension tests were carried out in the longitudinal, transverse, and bias (45° to the longitudinal axis) directions, until the tissue failed. Failure occured by sudden fracture; most often, fracture occured by rupture of the collagen-ossicle interface.

Stress vs. deformation plots of all tests were very linear. For a fibrous composite containing large holes, the dermis is surprisingly strong (Table 1). Part of its strength is probably due to the excellent bonding between the fibrous and ossicular components, and to the tight connections between fiber tracts. Most orthogonal materials are considerably weaker and less stiff on the bias, but this does not apply to the starfish dermis. Movement of the fibrous array on the bias is limited since the ossicles prevent the meshwork from collapsing. The fibers do not slip past one another when strained. Thus, the asteroid dermis provides a model for materials which can be easily bent or torted, but which will not deform in other directions.

TABLE 1

Stress Direction	Ultimate Tensile Stress, MNm^{-2}	Ultimate Tensile Strain	Young's Modulus, MNm^{-2}
longitudinal	37	.117	311
transverse	43	.146	397
bias	45	.116	446

AN EXPERIMENTAL STUDY OF THE CENTER AND ANGLE OF ROTATION OF A JOINT

Manohar M. Panjabi; Stephen Schick and Stephen Walter

Section of Orthopaedic Surgery, Yale School of Medicine
333 Cedar Street
New Haven, Connecticut 06510

Kinematic analysis of a body joint provides important information regarding the joint function. Center of rotation (CR) represents this information in a concise and convenient manner. The center of rotation provides useful information. It can help separate a de-arranged and diseased joint from the normal. Its knowledge is essential for replacement of a diseased joint by prothesis. Further, such information is also required in the determination of the joint loads. However, the CR is a sensitive quantity which is highly affected by errors in the measurement techniques. This is probably the main reason for the inconsistencies observed in the results of one and the same joint obtained by different researchers.

The purpose of the present study was to determine the errors in the measurements as well as in the location of the CR in a well defined and controlled experiment.

Our study is concerned with the common photogrammetry method of making measurements and Reuleaux analysis of data for the determination of the center of rotation. The experimental set-up consisted of two 6.25 mm Plexiglass plates joined together by a 12.5 mm cylindrical pin. The lower plate was fixed while the upper plate could be rotated about the center of the pin. Two points were placed on the fixed plate to define a fixed coordinate system. Forty-eight points in different directions and at different radii were placed on the rotatable plate. The rotatable plate was rotated and fixed in twelve different positions. The set-up was photographed in the initial positions and at each of the twelve positions. The photographs were projected onto the screen of a digitizer and coordinate measurements of all the fifty points were recorded by the computer. The digitizing process was repeated twenty times.

Calculations of a CR of a step of motion requires coordinates of two points in two different positions. Computer programs were written to calculate the CRs and angles of rotation for various pairs of points and several different combinations of positions. Means and standard deviations were computed to document the spread of errors in the coordinate measurements, the locations of the CRs and the angles of rotations. Graphs were plotted of the error-spread in the CR as functions of various parameters defining a planar motion-step.

Preliminary results indicate that there is a magnification of input errors. In other words, if the standard deviation of the measured coordinates of the points is σ_i, then the standard deviation of the center of rotation is several σ_i. Furthermore, it was found that this magnification is a function of many different experimental parameters. Results help us to optimally design our CR study experiments and to obtain best possible results for a given quality of coordinate measuring equipment. We hope that consequently more precise knowledge about the CRs of the human body joints will be obtained in the future.

"Mechanical Considerations in the Coordination of Sequential Joint Actions"
by C.A. Putnam, Biomechanics Laboratory, Department of Physical Education, University of Iowa, Iowa City, Iowa 52242.

Coordination in human movement implies specific patterns of muscle activities in terms of onset times and relative magnitudes. These patterns are expressed, within imposed mechanical constraints, in the motions of the body segments. One can often observe, in skills with similar performance criteria, characteristic patterns in the motion-time histories of the segments. The level of success in the performance of such skills is dependent, to a large extent, on the precise manner in which the movements of each segment are related to, or coordinated with, those of other segments.

The purposes of this investigation were: 1) to describe in detail the mechanical characteristics of two general, planar,two-segment motions, and 2) to investigate the effects that changes in selected aspects of the segment motions have on the resulting performance. Each general motion chosen for the analysis was characterized by a definite sequencing of the segmental motions. Each was represented by specific skills which clearly demonstrated this sequence in the motion of two adjacent segments. The first motion, typically found in skills in which an object is projected, was represented by a planar kicking action. In this skill, the forward motion of the leg is initiated by that of the thigh. Peak angular velocity of the thigh is realized well before that of the lower leg and of the peak linear velocity of the foot. The second motion, typically found in skills in which the movements of free limbs contribute to the movement of the body as a whole, was represented by a somersault dismount performed from an inverted pike position on the parallel bars. This movement is initiated by a rapid extension of the hips which precedes any large increase in the angular velocity of the remainder of the body.

Experimental film data were collected for 6 subjects performing the somersault dismount and 18 subjects performing a planar kick. These were analysed to determine the interaction between the two segments in terms of the forces and torques acting on each segment and the manner in which these interactions were expressed in the movement kinematics and angular momentum relations of the two segments. A series of motions were mathematically simulated to determine how the system might function within kinematic and kinetic constraints normally imposed on its motion. Boundary values for these constraints were derived from the experimental data. The results from the simulation revealed several specific aspects of the timing of segmental actions which were critical to a high level of performance.

THE EFFECTS OF HARD AND SOFT SURFACE WALKING ON SHEEP KNEES

Eric L. Radin*, Ronald B. Orr°, Jon L. Kelman+, Susan L. Schein°, and Robert M. Rose**

The purpose of this investigation was to determine the relationship between the resiliency of walking surfaces and corresponding changes in the femoral-patellar joint as monitored by hexosamine analysis of the articular cartilage and stereological evaluation of the trabecular bone.

Three adult sheep were subjected to 2 hours per day of slow steady walking on a concrete floor for a period of 20 months, and when not walking were kept on a blacktop surface. Two control sheep were walked in a similar fashion on a soft surface of wood chips. When not walking these animals were kept in a pasture.

X-rays of the experimental (hard surface) joints showed no evidence of osteoarthrosis, as indicated by the absence of joint narrowing, subchondral sclerosis, or osteophyte formation. Upon sacrifice, Meachim's grade II and III fibrillation was noted in the knees of the experimental animals.

In the experimental group, hexosamine analysis of the articular cartilage revealed a loss of proteoglycan in the weight-bearing regions. Hexosamine levels in the control group showed no loss of proteoglycan.

Stereological analysis of the distal femoral subchondral bone showed dramatic changes in the trabecular architecture. There were profound changes in trabecular volume, orientation, and contiguity with increased cortical thickening in the experimental group. A new orientation of the trabeculae in accordance with Wolff's Law occured with trabecular trajectories realigning themselves along the lines of increased stress.

The results suggest that walking on a hard surface has an adverse effect on the biochemistry of the weight-bearing articular cartilage and a significant change on the architecture of the underlying bone. These changes are frequently recognized clinically as an early indication of osteoarthrosis.

*Mt. Auburn Hospital
330 Mt. Auburn St.
Cambridge, Ma. 02138

°Museum of Comparative Zoology
Harvard University
Cambridge, Ma. 02138

+Children's Hospital Medical Center
300 Longwood Ave.
Boston, Ma. 02115

**Massachusetts Institute of Technology
4-132
Cambridge, Ma. 02139

IN VITRO MECHANICAL CHARACTERISTICS OF HUMAN SKIN WITH PARTICULAR REFERENCE TO RADIOTHERAPY EFFECTS

by

Harcharan Singh Ranu
Wayne State University, Detroit, MI 48202

Ionizing radiations have been used extensively in the treatment of malignant disease and the fact that skin tolerance has in the past limited the magnitude of the dose that can be administered in radiotherapy. Therefore, this study was undertaken in order to evaluate the influence of radiotherapy on the mechanical behaviour of human skin.

Irradiated and unirradiated post-mortem skin was obtained from female patients who had undergone a course of radiotherapy for the breast. The specimens were prepared and tested in a specially designed in vitro apparatus which was arranged on the Mayes hydraulic servo-controlled testing machine. The rate of loading used was 0.25 mm/sec. The perspex immersion tank was filled with normal saline solution at 37^{o}c and the specimen was allowed to equilibrate in fluid. A tensile load was imposed on the skin sample. Load against extension characteristics of skin up to rupture were recorded on the X-Y recorder. The results show that load - extension curve exhibits two portions which are identified with the alignment of the collagen fibers and then their subsequent stretching. The mechanical properties associated with fibre alignment are little affected by radiotherapy but the stiffness of the collagen itself tends to decrease with increasing dose. Similar trends have also been observed for rat and mouse skin*.

---

*Ranu, H. S. (1975). Effects of Ionizing Radiation on the Mechanical Properties of skin. Doctoral Thesis, CNAA, London, England.

In Vivo Echocardiographic Determination of Age Related Change in Elastic Stiffness of Ascending Aorta

Gautam Ray and D. N. Ghista
Department of Mechanical Engineering and Engineering Mechanics,
Michigan Technological University, Houghton, Michigan

K. B. Chandran, Div. Mat. Engg., Univ. of Iowa.

T. D. Giles, Dept. of Medicine, Tulane Medical Center, New Orleans.

The concept of changes in the elastic stiffness of the cardiovascular structures with age is well established. The terms such as "aortic hardening" etc. are used to qualitatively describe this change in the elastic property. Recent advances in the echocardiographic technique afford time dependent deformation imaging of the human ascending aorta. From this time dependent deformation data we have directly computed the elastic stiffness property of the ascending aorta and thus established a quantitative method to study the changes in this property with age and progression of the disease.

The flow chart below outlines the scheme the methodology:

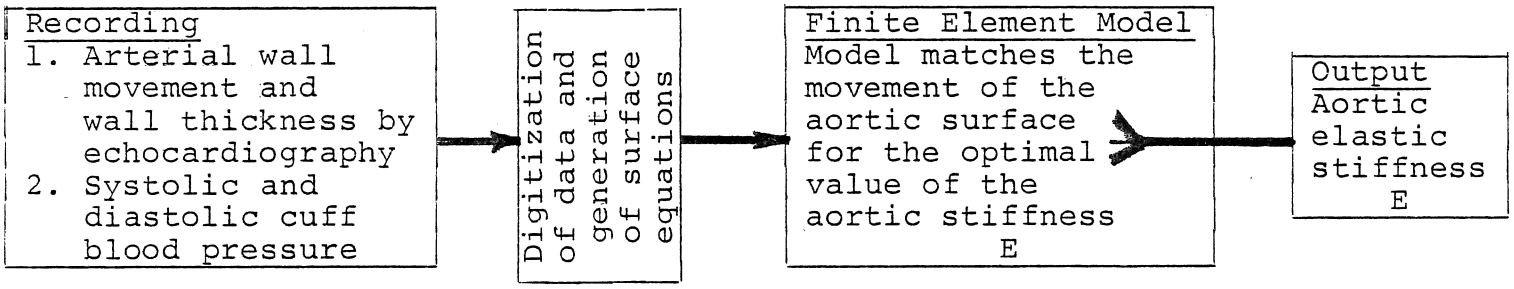

The following figure shows the nondimensional elastic stiffness of the ascending aorta of two patients during a cardiac cycle. The quantitative difference in the stiffness may be noticed.

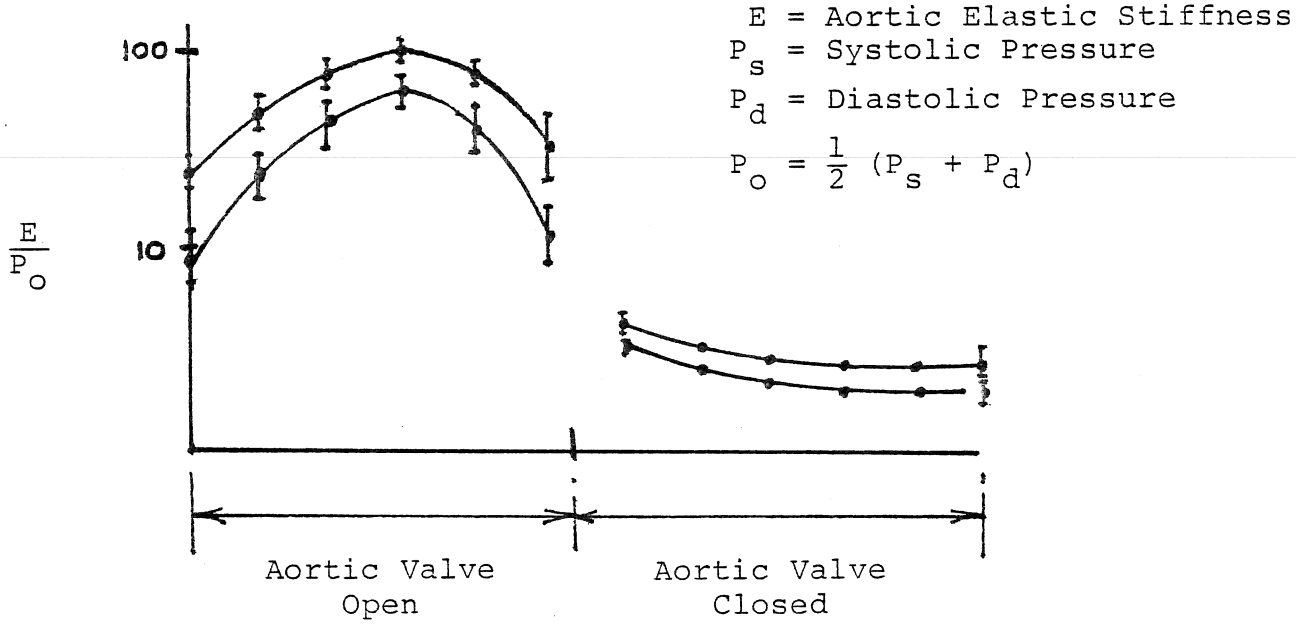

THE EFFECTS OF DIFFERENT GROUND SURFACES ON EQUINE JOINT MOTION AS ANALYZED BY ELECTROGONIOMETRY.

Judith Diana Ray,
Assistant Professor,
West Chester State College
West Chester, Pa.

The purpose of this investigation was to determine if there were differences in angular joint motions of horses moving over different hard and soft surfaces. Both carpus and metacarpophalangeal joints of the forelimbs were examined using electrogoniometry. Two male and four female Thoroughbred horses were used as subjects in the investigation. These clinically sound horses were led over six surfaces (concrete, grass, asphalt, woodshavings, hard dirt, and loose dirt) at a walk and trot. Oscillograph recordings were obtained and analyzed with the use of a computer.

Displacement and velocity curves were quantitatively and qualitatively analyzed. The joint motion of both the carpus and fetlock at a trot showed increased amplitude and decreased total time when compared with the walk. The start of carpus flexion was earlier, and extension later on loose dirt and woodshavings than on the other surfaces. Amplitude and air time were also greater. The goniograms of all surfaces had similar negative and positive slopes, amplitudes, and curve patterns. In angular velocity the greatest intersurface variation of joint motion occurred during the air phase on all conditions. This investigation provided needed information about the joint motion of horses moving on different surfaces. Knowledge of these detailed movement characteretics may contribute to injury prevention.

Estimation and Measurement of Loads on the Lumbar Spine

A.B. Schultz, G.B.J. Andersson, R. Örtengren, and A.L. Nachemson, UICC, Box 4348, Chicago, Ill. 60680 and Sahlgren Hospital, Gothenburg, Sweden.

Background: To achieve a more complete understanding of the relationship between physical activity in humans and pathologies of their lumbar spines, knowledge of the loads produced on the component structures of the trunk by different physical activities is required. The loads can be estimated through use of simple biomechanical models, but the validity of the assumptions made when using this approach need to be tested. Direct measurement of these loads in-vivo is impractical. Indirect experimental indicators of load can be used; these include measurements of surface myoelectric activity and intradiscal pressure measurements. In a series of analyses and experiments, we made model-based estimates of the loads, and tested the estimates with measurement of these experimental variables.

Methods: A wide range of isometric standing and seated activities were analyzed and corresponding experimental measurements made. Internal loads were predicted from equilibrium considerations on a statically-determinate basis when possible, or by use of simple optimization techniques when not. Appropriate segment weight distribution data were assumed; configuration data were gathered experimentally. Surface myoelectric activity was measured at twelve location in ten subjects, and in three additional subjects, intra-discal and intra-gastric pressures were measured as well.

Results and Conclusions: Good agreement generally was found between the predicted muscle contraction forces and the myoelectric signal levels, and between the predicted spine compression forces and the intradiscal pressure levels. The results imply that the loads on the spine can be adequately predicted using simple biomechanical models, or can be experimentally determined from the indirect measurements. The major determinant of the load on the spine is the net reaction moment created by the weights of the body segments superior to the lumbar region and by the other external forces applied to the upper body. In the isometric activities studied here, antagonistic muscle activity seemed to be minimal.

ANALYSIS OF REGIONAL FILLING AND EMPTYING IN THE LUNG

W.R. Scott and D.B. Taulbee, Department of Engineering Science,
State University of N.Y. at Buffalo, Buffalo, N.Y. 14214

Nonuniform ventilation distribution of inspired gases into the lung has been experimentally observed using radioactive tracer gases and external counters (1). For instance, at lung volumes near the residual volume, upper lung regions expand proportionately more than lower regions resulting in most of the inspired air going to the upper regions. Nonuniformities in the ventilation distribution and in the ensuing regional emptying pattern are also observed in the features of the single-breath washout curve graphing the tracer concentration versus expired volume.

These differences in the ventilation pattern have been theorized to be caused by regional differences in static transpulmonary pressure and that the pleural pressure gradient is related to gravity. It was observed (2) that the magnitude of the pleural pressure gradient in dogs was consistent with the hypothesis that air-filled lung tissue has the properties of a homogeneous fluid of the same mean density as the lungs. In this paper we expand on the above ideas and show, through the use of analytical models, that the idea of a fluid like behavior of the lung tissue under hydrostatic conditions is consistent with experimentally observed ventilation distributions and washout curves.

Assuming the lung is supported primarily by the pressure difference between the pleural space and the alveolar gas, a simple hydrostatic equation is derived which equates the vertical transpulmonary pressure gradient to the specific weight of the lung tissue. With conservation of tissue mass in a section of the lung the tissue density is related to the transpulmonary pressure through a fractional static volume/pressure curve. The lung parenchema is assumed to be homogeneous and, hence, described by one characteristic curve. Given the geometric shapes of the lung surface these relations can be solved to give the vertical tissue displacements relative to a reference state, the pressure and density variations, and the regional volume expansion. Results from this simple theory for the tissue displacements compare favorably with the results in (3) where the three dimensional large deformation equations of elasticity are solved using finite element numerical methods.

A geometric model was chosen to approximate the shape of the lung and the transpulmonary pressure distribution and the tissue displacements for this configuration are computed. A breathing maneuver is simulated by changing lateral model dimensions to reflect chest expansion and the length to reflect diaphragm displacement. At successive times through the breath the tissue displacements are computed and regional volume changes determined. With this information the distribution of an inspired bolus of tracer gas and the ensuing washout are simulated. Close agreement with the measurements in (4) infer the plausibility of the assumptions.

1. Milic-Emili, J., J.A.M. Henderson, M.B. Dolovich, D. Trop, and K. Kaneko. J. Appl. Physiol. 21:749-759, 1966.
2. Krueger, J.J., T. Bain, and J.L. Patterson, Jr. J. Appl. Physiol. 16:465-468, 1961.
3. West, J.B. and F.L. Matthews. J. Appl. Physiol. 32:332-345, 1972.
4. Robertson, P.C., N.R. Anthonisen, and D. Ross. J. Appl. Physiol. 26:438-443, 1969.

MECHANICAL RESPONSE OF BONE WITH AGE

P. A. Torzilli, K. Takebe*, A. H. Burstein and K. G. Heiple+

Biomechanics Department, The Hospital for Special Surgery,
535 East 70th Street, New York, New York 10021

INTRODUCTION

Deformation beyond the elastic limit in whole bone produces nonlinear yielding without the consequence of fracture. This phenomena is most often observed in young children after trauma, where a large permanent deformation of a long bone is possible without any radiographic evidence of bony fracture. This mode of failure is quite different from the partial splinter fractures known as Greenstick fractures. Mechanical testing of whole bone in bending will yield the characteristic response of bone as in the in-vivo situation. This type of testing readily yields the moment (load) carrying capacities and resulting deflections in both the linear and nonlinear regions. These properties change with bone age and form the bases of the physiological responses found in clinical situations. This investigation is concerned with the variation with age in the structural and material properties of canine bone.

MATERIALS AND METHODS:

Twenty-two dogs of similar breed from four different litters were sacrificed at ages ranging from one week up to 14 months. In all one hundred bones were obtained for mechanical testing; 34 tibia and femora, 11 radii and ulnae, and 10 humeri. The tibia and femora were tested in both three and four point bending. Radii, ulnae and humeri were tested in three point bending. Each bone was loaded up into the nonlinear region until either a zero slope in the load-deflection curve was reached or failure occurred. Those which did not fail were unloaded in order to calculate a residual deformation. In matched pairs of tibia and femora of 2 months and older, one bone was tested in either three or four point bending, and the other bone was sectioned for determination of cross-sectional geometry and material properties.

RESULTS:

Material property tests demonstrated the usual stress-strain curve characteristics of cortical bone, i.e., linear elastic response followed by a nonlinear permanent deformation region. The elastic modulii in tension and compression became progressively higher with age, while the nonlinear modulii slope remained somewhat constant.

Bending tests showed an initial linear region followed by a non-fracture nonlinear region. Large permanent deformations were found, with increasing nonlinear deformation with decreasing age. In all bones the flexural rigidity increased with age exhibiting increased load carrying ability and decreased deflection.

* Kobe University School of Medicine, Kobe, Japan
+ Case Western Reserve University, Cleveland, Ohio

GEOMETRY OF AIRWAYS and DIFFUSIVE GAS MIXING IN THE LUNG. H. D. Van Liew and K. R. Murray. Department of Physiology, State University of New York at Buffalo, New York, 14214.

Variability of mechanical properties of tissue from one lung region to another can lead to marked inefficiency of gas exchange. Prior to study of such effects, however, we needed to identify the important variables that govern the amount of inspired gas that becomes mixed with resident gas in a homogeneous lung or along a single pathway of a heterogeneous lung.

According to Weibel's morphometric data, there is a vast increase of summed cross-sectional area and decrease of length of lung airways between trachea ($i = 0$) and the terminal alveolar exchange units ($i = 23$ for 23 generations of branching). We calculated a "diffusive time constant" from airspace volume, airway length, summed cross-sectional area, and gas-phase diffusivity (V_iL_i/DA_i); it was less than 0.1 sec for all but the uppermost airways, whereas duration of a breath is several seconds. Because of the short time constant, all of the lung gas except that in uppermost airways equilibrates rapidly if diffusion proceeds unhindered, as in a breathhold.

During inspiration, convective flow moves inspired gas through the airways until it reaches the generation in which diffusive conductance, DA_i/L_i, equals convective delivery; just beyond that generation, there is a steep gradient between pure inspired gas and the "alveolar" gas in the rest of the lung. When convective flow slows and stops so that expiration can occur, the diffusive process reverts to a "breathhold mode," in which the steep gradient recedes toward the trachea until it is practically stopped in the upper airways with long time constants.

The lung is well constructed to maximize amount of inspired gas that becomes mixed with resident gas in one breath. Diffusive processes are so strong that mechanical mixing probably has little overall effect. Shortening of time for diffusion (exercise), variability of lower airway geometry (disease), and decreasing the gas-phase diffusivity (hyperbaric environments) will all be manifested as changes in amount of inspired gas that remains in the uppermost airways that have long time constants. The capacity of these upper airways is small, so changes of amount of gas in them is of minimal consequence to overall gas exchange. (Supported in part by NIH Grant PO1 HL14414.)

"An Alternative Method for the Calculation of the Resultant Forces and Torques Acting at Human Joints", by C.L. Vaughan, Biomechanics Laboratory: Department of Physical Education, University of Iowa, Iowa City, Iowa 52242.

Ever since the pioneering work of Braune and Fischer, biomechanics researchers have been interested in the inverse dynamics problem: the calculation of kinetic parameters from experimentally recorded displacement-time data of human movement. Up until the present time, the determination of these parameters appears to have been accomplished by the same standard procedure (1,2). The kinematics of a distal segment are incorporated in Newton's Second Law to evaluate the force and torque acting at a joint connecting proximal and distal segments. It is then possible to progress sequentially, determining the kinetics at each subsequent joint. This method can only be utilized when the distal segment is free to move in space or is in contact with a surface and the interacting force and torque are known (e.g. the foot on a force plate). Limitations exist when a closed loop is formed by two distal extremities in simultaneous contact with an external system and no force-transducing device is available to monitor these contact forces.

Quite recently, engineers concerned with the dynamic analysis of machinery and mechanical systems (3,4) have developed general purpose and user-orientated computer codes. While these codes are specifically designed to study the forward dynamics problem (predicting the kinematics from known kinetic functions), they can be adapted to solve the inverse dynamics problem for the study of human movement. The location of each rigid body segment in 3D space is specified by 6 generalized coordinates, and the dynamic system of equations for an individual body is formulated using Lagrange's equations of motion. In addition, a number of constraint equations are required: (a) to specify the geometry of the joints (e.g. revolute, spherical, universal), and (b) to specify the displacement-time history for each rigid body in the system. Each constraint equation has an associated Lagrange multiplier which, in physical terms, is equivalent to a joint force or torque. The solution of this large system of differential and algebraic equations is achieved using an efficient numerical integration technique. The joint forces and torques are therefore solved simultaneously rather than in the sequential fashion of the Newtonian approach.

In order to compare the two methods, a simple planar arm-swinging action was studied. The angular orientations of the upper arm and forearm were measured at consecutive instants and these kinematic parameters were used to calculate the forces and torques at elbow and shoulder joints. The force values varied from -40 to 60 N (difference between methods was no greater than $\pm$2 N) and the torques ranged from -2 to 15 Nm (difference $\pm$1 Nm). The Lagrangian approach combines reliability with versatility, and can handle the situation where the force on a distal segment is unknown. It is therefore felt that this procedure has great potential and should be developed and extended in the future.

References

(1) Aleshinsky, S.Y. and V.M. Zatsiorsky, J. Biomechanics, 11:101-108, 1978.
(2) Andrews, J.G., Kinesiology III, AAHPER, 1973.
(3) Haug, E.J. et al, Technical Report 50, U.S. Army, Warren, Michigan, 1978.
(4) Paul, B., Mechanism and Machine Theory, 10:481-507, 1975.

Life in a Velocity Gradient

Steven Vogel
Department of Zoology
Duke University

Let's begin with two rather ordinary observations, one biological and the other physical. First, almost all organisms are very much smaller than we - whether in number of individuals, number of species, or total mass, we're in the most extreme 1%. Second, whenever fluid flows over a solid surface, the fluid at the surface is stationary. Thus a region exists near any surface in which the speed of flow gradually and asymptotically increases from zero to the full "free stream velocity" at some distance from the surface. The outer limit of this region is, of course, an arbitrary convention: the common limit of 99% of free stream velocity is just an accident of our bipedal and pentadactylic lineage. In practice, then, this "boundary layer" of semi-stagnant fluid forms a fuzzy cloud on the surface of any object in motion with respect to any fluid.

How are size of objects and the dimensions of boundary layers related? For a flat plate oriented parallel to the direction of (laminar) flow, the thickness of the layer is proportional to the square root of the distance downstream from the upstream edge of the plate - the boundary layer thickens, but more and more slowly, as one proceeds downstream. And the average thickness of a boundary layer, relative to the size of an object, will be greater for a small object than for a large one. In addition, thickness is inversely proportional to the square root of velocity. If, as seems common, small organisms move more slowly than large ones, they will be immersed in an even more disproportionately thick boundary layer. Furthermore, even if a small organism doesn't move but merely sits on some surface in a moving fluid, the relation between its size and the thickness of a boundary layer is of consequence - it is likely to be totally immersed in the boundary layer on that surface. In short, for an organism of a more biologically ordinary size than we, free stream velocity may have as little direct relevance as do the stratospheric winds to us. Such an organism cannot move without carrying a large clound of fluid and, if attached, is "automatically" shielded from the full force of ambient currents.

The combination of our two initial observations proves to be rich in biological implications. The major portion of the talk will consider a few relevant situations as a stimulus, perhaps, to a less anthropometric view of adaptations to the physical world. We'll consider the necessity of protruding well up from a surface if one is to filter food borne by currents as well as the difficulty of designing a micro-filter where the boundary layer of the mesh tends to occlude the pores - scale down a sieve and it will eventually do duty as a bucket. We'll view boundary layers as thermal insulation and use that notion to relate the shapes of leaves to their positions and orientations on trees - if you're an unscalloped leaf, don't let the sun catch you horizontal. We'll be concerned about the actual mass of fluid carried along on small organisms in motion, noting that for some it may be of similar magnitude to body mass - for a small, flying insect, air is a sort of rarified mud. And finally, we'll recognise that a boundary layer is a region of energy degradation, but that a little of that energy can be diverted to more bioportentous ends, reducing the cost of living for a variety of craspedophilic creatures living at the interface between solid and moving fluid.

The fluids of interest are, of course, air and water; their behavior is surprisingly similar from the point of view of organisms. At ordinary temperatures, similarity of flow pattern (and thus thickness of boundary layers) if wind speeds are about fifteen times greater than water currents. Coincidentally, airflows in nature are about that much faster than the flows of water: one meter per second is a moderate current of water while fifteen is a moderate wind. Twice either is a torrent or storm.

SHARK BACKBONE: STRUCTURE AND FUNCTION

Steve Wainwright
Zoology Department
Duke University, Durham, N. C. 27706

A previously undescribed intervertebral mechanism occurs in sharks and is causing us to reconsider how sharks swim. The vertebrae of dogfish and carcharinid sharks have biconcave centra consisting of calcified cartilage with radial inclusions of noncalcified cartilage in the midsection. Calcified cartilage is present in two textures: a less dense one in the midsection of the centra and a denser one covering the ends.

The intervertebral tissues comprise a liquid-filled capsule of dense basophil connective tissue that is firmly attached to the ends of the centra. It is finely fibrous material and it extends outward radially so as to prevent adjacent centra from touching, even in tight bending. Encircling this gasket is a ring of hyaline acidophil material that appears amorphous by direct microscopy. These tissues, structures and fluids are apparently undescribed in the literature.

The entire backbone is wrapped in a multilayered tunic of collagen fibers that are visible to the eye. These fibers lie in right- and left-handed helices around the backbone and are continuous with midsaggital septa and horizontal septa in the fish's body.

I measured the force required to bend whole, dead sharks into arcs of decreasing radius of curvature (R). Arcs of R = 38 cm (observed in slow swimming sharks) require 1/2 to 1/3 as much force as arcs of R = 20 cm (observed in fast swimming sharks). About 1/10 of the force required for the fast swimming R = 20 cm is required to bend just the backbone and its investing connective tissues. All bending deformations in backbones and in whole fish are recovered upon unloading.

This information indicates that the elastic stiffness of shark backbones, like that of the skin, rises with the increase in deformation observed between slow and fast swimming. The intervertebral structures described here and the helical wrappings of collagen fibers appear to be responsible for this modulatable spring in the shark's backbone.

THE RECOGNITION AND CORRELATION OF HUMAN MOVEMENT PATTERNS

W. C. Whiting, R. F. Zernicke, T. M. McLaughlin, and R. J. Gregor
Biomechanics Laboratories, Department of Kinesiology, University of California, Los Angeles, California, and Auburn University, Auburn, Alabama

A key element in the analysis of kinematic and kinetic data derived from human movement studies is the determination and establishment of a quantitative measure of the equivalence between two patterns. Typically, segmental motion data are plotted as functions of time or as parameter versus parameter, e.g., angle-angle graphs. When no composite description is required, minima, maxima, or derivatives of the curves may suffice. If, however, the description of a pattern's shape or the determination of the degree of matching between two patterns is desired, discrete point by point comparisons may prove inadequate.

In the field of pattern recognition, methods of shape description have been developed for applications ranging from analysis of simple line drawings to complex image processing. Of the numerous techniques available, we have found the chain encoding method (1) to be a viable means for shape description and pattern comparison in human motion analyses. The method consists of the quantization of curves and shapes in a square lattice of of sufficient fineness to maintain the details of the contours and encoding in terms of the 8-direction chain code. Once two patterns have each been encoded as a series of integers, it is possible to examine the degree of correspondence or coherence between the patterns. Cross-correlation functions can be calculated to derive a recognition coefficient, R_{ab} (the peak value of the cross-correlation function). This recognition coefficient indicates the degree of coherence between the two patterns, with unity indicating a one-to-one correspondence.

We have found the combined chain encoding and cross-correlation algorithms to be effective for detecting variations and abnormalities in human movement. In the case of gait pattern analysis, figures 1, 2, and 3 depict the thigh angle versus knee angle diagrams for a normal adult walking at 4.8 km/hr (Fig. 1), normal adult running at 11.5 km/hr (Fig. 2), and the normal limb of a unilateral above-knee child amputee. With appropriate encoding and scaling, the pairwise cross-correlations were determined to be: $R_{12} = 0.75$, $R_{23} = 0.41$, and $R_{13} = 0.56$. The strength of the cross-correlation thus indicates the coherence between the movement kinematic patterns.

(1) Freeman, H. A technique for the classification and recognition of geometric patterns. Proc. 3rd International Congress on Cybernetics, (Namur, Belgium), pp. 348-369, September 1961.

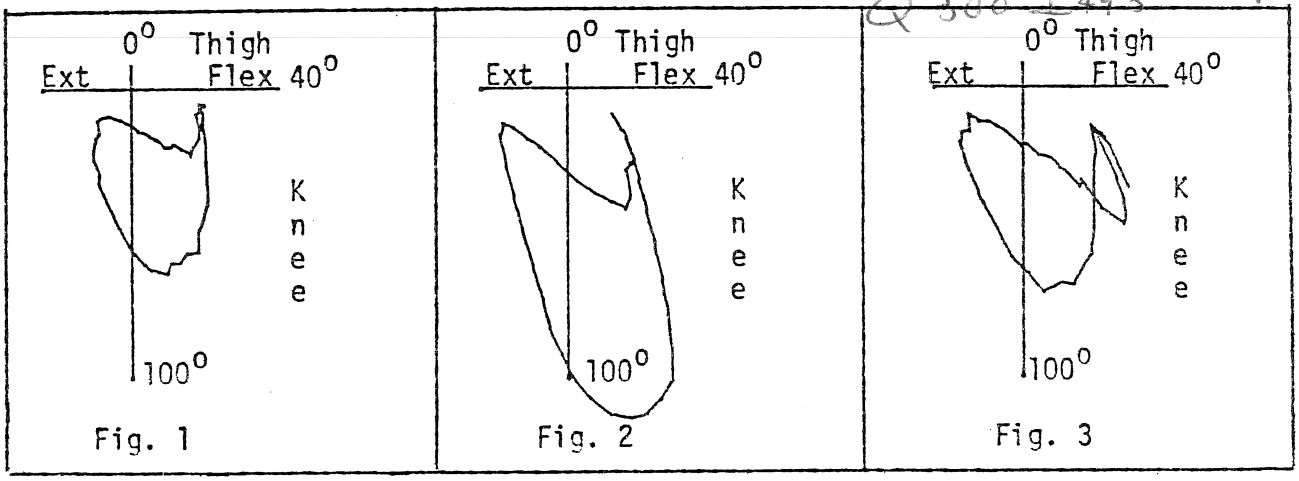

Fig. 1 Fig. 2 Fig. 3

LOAD-RESPONSE CHARACTERISTICS OF THE LUMBAR SPINE

M.A. Wilson, R.D. Crowninshield, R.A. Brand, T.R. Lehmann

Orthopaedic Biomechanics Laboratory
University of Iowa, Iowa City, Iowa

A method of investigation into the contribution of various constituent structures to the kinematic response of isolated lumbar spine specimens has been developed. Fresh lumbar spines (T12 through S1) and surrounding soft tissue structures were tested intact and after alterations intended to reproduce conditions of tissue degeneration, injury, and surgical alteration. The spine's response to loads producing a flexion moment and compression, an extension moment and compression, and a flexion-twist moment and compression were recorded. Three non-colinear externally visible reference markers were attached to L1, L2, L3, L4, L5, and S1. The sacrum was cast into an acrylic plastic for mounting on a loading table and a loading rod was fixed to T12. Biplanar x-rays of the specimen with the external markers were taken in a calibration cage. An internal reference frame was chosen in each vertebra based on bony landmarks seen in the 45-degree oblique x-rays. The external markers and the bony landmarks of each vertebra were digitized for computer analysis which defined external and internal reference frames. The analysis provided the displacement and angular orientation of each external reference frame relative to the internal reference frame of the vertebra to which it was attached. Biplanar photographs were taken of the specimen mounted on the loading table. Loads of constant magnitude and orientation relative to the sacrum were applied through the loading rod by pnuematic cylinders. Two minutes after each load application another set of biplanar photographs were taken to record the displacement of each vertebra's external markers. Analysis of the film permitted the determination of the spatial position and orientation of each vertebra's internal reference frame from the location of the external reference frames. After recording the initial load response, alterations were produced in the specimen such as various techniques of surgical decompression. The altered specimen's response to the loading was recorded to permit an analysis of the constraining role of the resected structures.

Pattern of Joint Moments During Stance Phase of Gait

David A. Winter
Department of Kinesiology
University of Waterloo, Waterloo, Ontario

One of the most valuable assessment tools in gait is the time history of the net moments at each joint. One is therefore motivated to search the patterns of joint moment histories to see if basic patterns exist. A review of a number of papers that report these time histories during stance is quite revealing:

1. Of the 7 major papers reviewed there were only 8 case histories of moments at all three joints with 6 additional histories at the knee only.
2. Only the ankle joint has a consistently recognizeable pattern: a small dorsiflexion moment followed by a strong plantarflexor moment.
3. The hip has a less consistent pattern, usually extensor followed by flexor.
4. The pattern at the knee is quite inconsistent and unpredictable.

A review of these same patterns in 30 subjects and 9 patients assessed in our laboratory gave the same conclusions. In addition an anomaly became evident in several of the records: the presence of dominant or complete knee flexor activity during the entire stance period, and yet the knee angle history was quite normal. This led to the development of a principle of lower limb support. Collapse of the knee can be prevented by any combination of extensor activity at the hip, knee and ankle, as long as the algebraic sum is sufficiently positive. Assuming counter-clockwise moments to be positive, the net supporting moment $M_S = M_k - M_a - M_h$, where M_k, M_a and M_h are the moments at the knee, ankle and hip, respectively. To validate this principle M_S was calculated for all 39 trials. The pattern for M_S was seen to be basically the same in all cases, rising from a zero at heel contact to a peak and decreasing to near-zero or slightly negative at toe-off. In order to compare patterns all records were normalized in time so that stance period = 100%, and the maximum M_S was set at 100%. The M_S curve was then averaged over stance for similar groups. Two example curves are shown below, Figure 1 is the average of 3 different joggers, Figure 2 is an average of 12 different normals walking at a comfortable cadence. One standard deviation is shown as vertical bars. It appears that the basic pattern resembles the vertical force plate signal, indicating that all three joints of the lower limb co-ordinate their total muscular activity in response to the ground reaction force.

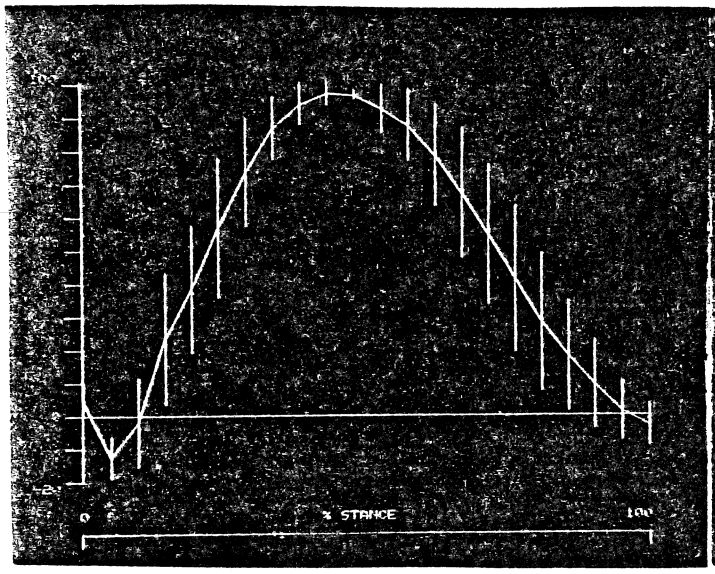

Fig. 1. Average of M_S for 3 joggers.

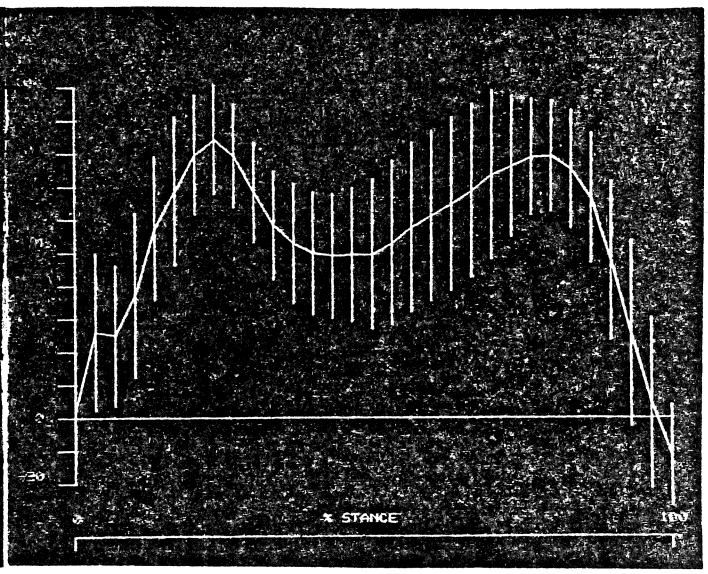

Fig. 2. Average of M_S for 12 normals walking at a comfortable cadence.

ANATOMICAL AND MECHANICAL PARAMETERS AFFECTING THE BUCKLING LOAD OF THE HUMAN SPINE -CLINICAL EVIDENCE IN IDIOPATHIC SCOLIOSIS

T. T. WONG, G. M. McNEICE, J. ROORDA and V. J. RASO
DEPARTMENT OF CIVIL ENGINEERING
UNIVERSITY OF WATERLOO
WATERLOO ONTARIO
CANADA N2L 3G1

In order to provide meaningful treatment schemes for idiopathic scoliosis, accurate prognosis of the likelihood of progression is essential. In order to define some characteristics of the spine which will contribute to such a progression, it is necessary to investigate the relative importance of the common factors affecting the load-deformation characteristics of the spine. In this paper a two degrees-of-freedom rigid link model of the adolescent thoraco-lumbar spine has been developed to study qualitatively the effects of these parameters. Figures 1 and 2 illustrate the model and the parameters. It is postulated that idiopathic scoliosis is initiated by the loss of the passive stability of the spine. This passive stability is due to the stiffnesses of the intervertebral joints and the attached muscles in a passive state (i.e. not being fired). The results from a series of buckling load analyses indicate that the ranking for nine important factors in a decreasing order of relative importance, is as follows:

1) Length Factor (ratio of thoracic spine length to thoracolumbar),
2) Body Weight Distribution (thoracic and lumbar regions),
3) Intervertebral Joint Stiffness,
4) Inclination of the lower back muscles,
5) Passive Stiffness of the lower back muscles,
6) Line of action of the upper trunk muscles,
7) Length of thoracolumbar spine,
8) Passive Stiffness of the upper back muscles,
9) Ratio of Joint Stiffnesses (between the thoracic and lumbar regions).

Application of this model to patients currently being studied at the Hospital for Sick Children in Toronto led to the indication that the Length Ratio parameter is an important consideration affecting the stability of the scoliotic spine. Table 1.0 presents Length Factor results for five patients for which final decisions have been made (thirty five patients studied). We observe that those requiring surgery have a greater Length Factor and that their factors increased with age rather than decreasing or stabilizing. Attempts to measure the other parameters clinically are underway at the Hospital for Sick Children.

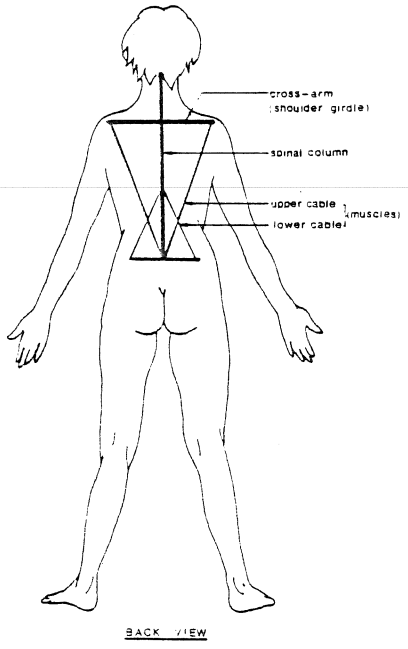

Figure 1.0

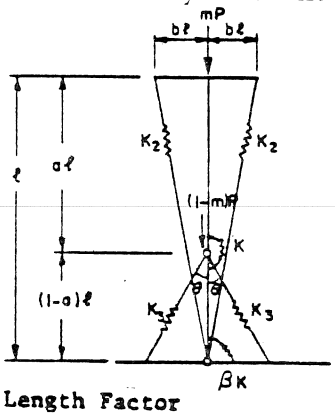

a: Length Factor
b: Cross-arm Factor
l: Overall Length
k: Rotational Stiffness
k2: Upper Cable Spring Stiffness
k3: Lower Cable Spring Stiffness
m: Load Distribution Factor
β: Stiffness Factor
ε: Initial Geometric Imperfection
θ: Cable Inclination

Figure 2.0

	PATIENT	AGE (Yrs)	LENGTH OF SPINE (cm) THORACIC	LUMBAR	OVERALL	LENGTH FACTOR	GROWTH RATE+	REMARKS
GROUP A	A04	12.50	237	134	371	0.639	insignificant	curve stabilized brace treatment stopped
		12.75	236	132	368	0.641		
		13.25	235	132	367	0.640		
		13.50	235	134	369	0.637		
	A11	14.75	259	146	405	0.640	insignificant	curve stabilized brace treatment stopped
		15.00	257	141	398	0.646		
		15.25	253	141	394	0.642		
	A12	16.00	234	136	370	0.632	insignificant	curve stabilized brace treatment stopped
		16.25	235	132	367	0.640		
		17.00	235	132	367	0.640		
		17.25	238	131	369	0.644		
GROUP B	A15	11.25	224	120	344	0.651	16	surgery required
		11.50	231	120	351	0.658		
		12.00	237	125	362	0.655		
		12.75	244	124	368	0.663		
	B14	8.50	196	108	304	0.645	24	surgery required
		9.00	203	112	315	0.644		
		9.25	211	109	320	0.659		
		9.75	205	110	315	0.651		
		10.00	226	114	340	0.665		

* overall length = thoracic length + lumbar length

+ growth rate = [final - initial (overall) length]/time (mm/yr

Average length factor for patients: 0.651 at 9.0 years
0.644 at 15.5 years

Table 1.0

Mechanical Energies in Overground and Treadmill Walking

Sandra M. Woolley, David A. Winter
Department of Kinesiology
University of Waterloo, Waterloo, Ontario

The treadmill has been used as a convenient means of evaluating performance in a number of diverse physiological situations. The direct extrapolation of data from treadmill to overground situations has been a point of contention. In terms of metabolic expenditure, some researchers (Ralston, 1960; McMiken et al., 1976) contend that no difference exists, while others report anamolous findings (Daniels et al., 1953; Custance, 1970; Nelson et al., 1972; Elliott and Blanksby, 1976). Little has been mentioned in the literature about the mechanical energies involved in either situation. This paper deals with that aspect of walking.

Six male subjects trained in treadmill walking were assessed for three successive strides. The filtered displacement data were processed to obtain kinematic histories of segment angles and centre of gravity. The analyses included the potential and kinetic translational and rotational energy components of each segment. A summation of all segmental components over time yields the segment total body energy, STBE, (Winter et al., 1976). An integration of the absolute value of the positive and negative energy changes over one stride gives WT_{wb}, the internal mechanical work, which takes into account any energy transfers within and between segments (Winter, 1979). The analyses were modified to sum across components but not across segments, thus the integration of the energy changes gives WT_w, which accounts for only the energy changes within segments. Finally, if we sum the absolute value of the energy changes in all segmental components we get WT_n, the work done had there been no energy exchange within or between segments. $WT_w - WT_{wb}$ now gives the magnitude of the energy transfers between segments and $WT_n - WT_w$ gives the energy exchanges within segments.

Results and Discussion

A comparison of WT_{wb}, WT_w and WT_n was made for both treadmill and overground conditions and no statistical difference was found. However, the stride-to-stride variability of all three work measures for the overground trial was significantly higher ($p<.05$). This finding suggests that the treadmill walking is a more rigidly controlled condition, while overground walking permits individual stride-to-stride variations. An additional indication of this variability is seen in the average STBE over three strides in Figures 1 and 2. It can be seen that the treadmill is quite consistent over the stride, whereas the variability persisted over the entire stride in the overground condition.

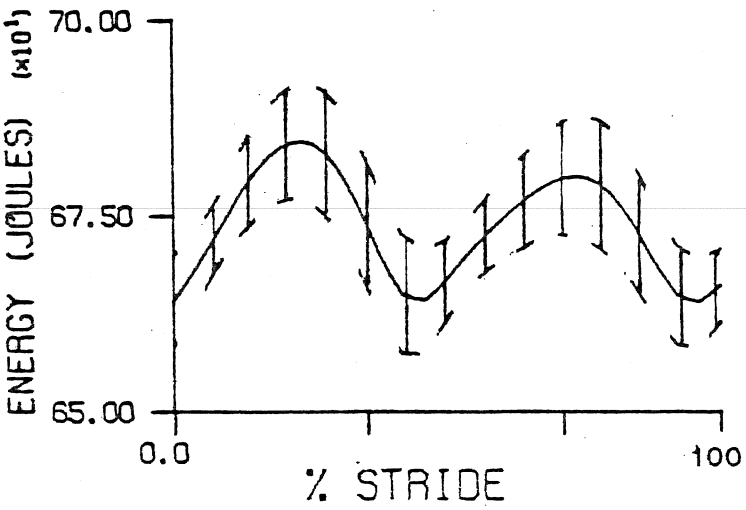

Figure 1. 3 stride average of STBE Overground

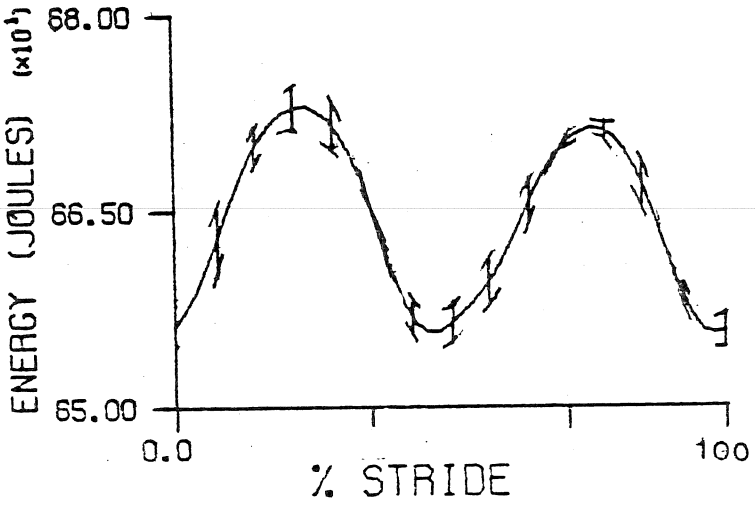

Figure 2. 3 stride average STBE Treadmill

THEORETICAL AND EXPERIMENTAL STUDIES OF SWIMMING BIOMECHANICS

Rachel Yeater, Bruce Martin, Kevin Gilson, Mary Kay White

Human Performance Laboratory/Orthopedic Research Laboratory

West Virginia University, Morgantown, WV 26506

We are studying the mechanics of competitive swimming in order to elucidate the determinants of performance and the musculoskeletal demands of this sport. Our approach is to combine experimental measurements with theoretical studies designed to reveal the relationships between experimental variables.

To date the experimental subjects have been 18 members of the WVU men's swimming team. The propulsive forces produced by these subjects during tethered swimming of the crawl, breast, and backstroke (and arm and leg components thereof) were recorded as functions of time using a load cell in the tether cable. The magnitudes and temporal patterns of each stroke were compared with performance (free swimming velocity), anatomical parameters, and technique as evaluated by the coach. The results demonstrate a variety of technique-related force patterns among the subjects. Fig. 1 shows typical crawl, back, and breast stroke records and respective mean forces for the team.

The theoretical results to date represent a simple model for the crawl stroke. They indicate that tether forces are considerably greater than propulsive forces generated during free swimming, a result not previously recognized in the literature (Fig. 2). Other observations are beyond the reach of a simple model, yet are intuitively predicted by coaches. For example, tether forces increase with stroke rate to a point, but then decline with excess arm velocity. Also, our data confirm the feeling held by most coaches that the flutter kick produces insignificant propulsive forces during the crawl stroke. In the breast stroke, on the other hand, the kick is the major force producer.

Contrary to the assumptions of previous studies, we have found that free swimming velocity does not correlate well with tethered swimming force. While velocity is somewhat affected by stroke rate, anatomy, and the ability to generate high tethered forces, as yet intangible attributes of technique appear to be major determinants of performance. Further research is being conducted to clarify these factors and to compare men and women swimmers.

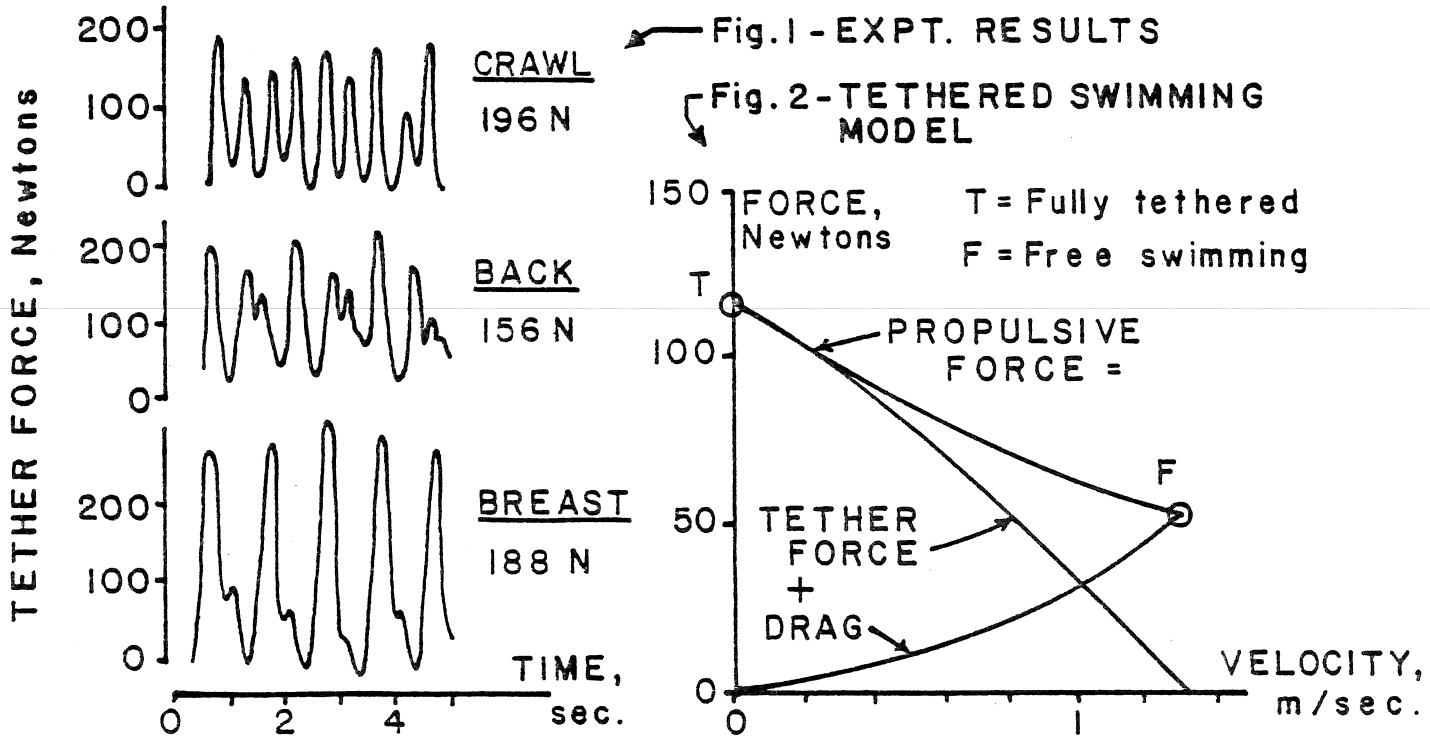

KINETICS OF SLOW AND FAST ANKLE EXTENSORS OF CAT DURING JUMPING

R. F. Zernicke, J. L. Smith, M. G. Hoy, and H. D. Stewart.
Biomechanics and Neuromotor Control Laboratories, Department of Kinesiology, and Brain Research Institute, University of California, Los Angeles, CA 90024

Variations in the kinetic demands placed on the musculoskeletal system elicit significant functional differences in synergistic fast and slow muscles. Little information exists, however, in which myoelectric (EMG), kinematic and kinetic data have been synchronously recorded to correlate neuromuscular and mechanical function in freely moving animals. We, therefore, have recorded EMG signals from slow (soleus) and fast (lateral gastrocnemius) ankle extensors in cats during vertical jumps to heights of 40, 60, and 80 cm. The chronically implanted cats were trained by food reward to jump from a force platform to the specified heights. Myoelectric signals from the muscles were multiplexed and transmitted on a single carrier frequency through a small PAM-FM telemetry transmitter that was attached to a connector mounted on the skull of the cat. The raw EMG (R-EMG) and the rectified-averaged (A-EMG, time constant = 50 ms) signals and the force platform data were recorded on FM tape for subsequent computer analysis. A motor-driven 16 mm camera (100 frames/s) was synchronized with the EMG and reaction force records. Figure 1 is an exemplar one second record of the vertical force (peak = 129 N) and the R-EMG of the LG and SOL for a 80 cm jump. The 100 Hz synchronizing pulse from the camera internal timing lights is shown on channel 4. Serial frames of each jump were projected and joint coordinates were digitized to determine the angular kinematics of the jump; digital filtering techniques were used to smooth coordinate data (cut-off = 7 Hz). Prior to the calculation of the hind limb joint moments of force, it was necessary to determine the segment masses, centers of gravity, and moments of inertia. Limb segment parameters for nine cats and total body segment information for four cats were determined and regression equations were developed to predict the necessary constants for the rigid body analyses of the ankle joint moments during the jumps.

Previous data (1) have highlighted the low tension producing capability and the postural role of the SOL and have proposed that the fast LG is recruited selectively as the kinetic demands significantly increase. The data of our present study support the notion that the significant increases in jumping height, from 40 to 80 cm, are closely associated with increased LG peak A-EMG, as well as peak ankle angular acceleration, reaction force maximum, and peak reaction force dF/dt.

(1) Smith, J. L., Edgerton, V. R., Betts, B., and Collatos, T. C. EMG of slow and fast ankle extensors of cat during posture, locomotion, and jumping. J. Neurophysiology, 40: 503-513, 1977.

FIGURE 1